μl. After incubation at 37 °C for 10 min, the reaction was stopped by the addition of 0.3 ml of chloroform/methanol (1:2, v/v). Total lipids were extracted using the Bligh-Dyer method (32) and subsequently analyzed by TLC in chloroform/methanol/acetic acid/water (50:25:8:4, v/v/v/v). Bands at positions corresponding to the expected product were visualized by I_2 vapor, cut from the plate, placed in Microscinti-O (Packard Bioscience), and analyzed in a liquid scintillation counter LS6500 (Beckman).

Radioligand Binding Assay—The method of PAF-PAF receptor (PAFR) binding assay was described previously (7, 33). Briefly, the membrane fraction containing 158 fmol of PAFR from hearts and skeletal muscles of PAFR transgenic mice (7, 34) were mixed with 25 nM [^{3}H]WEB 2086 and the lipid extract in a 96-well plate. After incubation at 25 °C for 90 min, receptor-bound [^{3}H]WEB 2086 was collected by filtration through a UniFilter-GF/C (PerkinElmer Life Sciences) using a MicroMate 196 simultaneous 96-well harvester (PerkinElmer Life Sciences), and the filter was washed and dried. Subsequently, the radioactivities were counted with a TopCount microplate scintillation counter (PerkinElmer Life Sciences).

Electrospray Ionization Mass Spectrometry Analysis of PAF—Extracted lipid from the acetyltransferase assay was identified by electrospray ionization mass spectrometry analysis. The analysis was performed using a 4000 Q-TRAP quadrupole-linear ion trap hybrid mass spectrometer (Applied Biosystems/MDS Sciex, Concord, Canada) with an Ultimate 3000 high pressure liquid chromatography system (DIONEX Co.) combined with an HTC PAL autosampler (CTC Analytics, Zwingen, Switzerland). The extracted lipids were subjected to electrospray ionization mass spectrometry analysis by flow injection without liquid chromatography separation. The solvent was acetonitrile, methanol, 50 mM ammonium formate, pH 7.4 (v/v/v, 45/50/5), and the flow rate was 10 μl/min. The scan range and speed were set at m/z 500–600 and 1000 Da/s, respectively. The trap fill time was set at 5 ms, and the ion spray voltage was set at −4500 V in the negative ion mode. Nitrogen was used as curtain and collision gas. The declustering potential was set at 20 V to minimize in-source fragmentation. Both Q1 and Q3 resolution were set to unit mass. The collision energy used was varied according to the desired experiment. The method to identify phosphatidylcholine species was described previously (35).

siRNA Transfection—hLysoPAFAT/LPCAT2 siRNAs (siRNA ID numbers 140446, 140447, and 140448; Ambion) and control siRNA (silencer negative control 1; Ambion) were transfected using siPORT amine transfection agent according to the manufacturer's protocol. The siRNA transfection was performed for 2 days in HEK293 cells.

Short Term LPS Stimulation—After transfection of RAW264.7 cells with LysoPAFAT/LPCAT2 using Lipofectamine 2000, cells were pretreated with or without 20 μM SB 203580 for 1 h and subsequently stimulated with 100 ng/ml LPS for 30 min. For preparation of cell extracts, the cells were scraped into 600 μl of an ice-cold buffer containing 20 mM Tris-HCl, (pH 7.4), 50 mM β-glycerophosphate, 1 mM sodium orthovanadate, 5 mM 2-mercaptoethanol, 20 μM 4-amidinophenylmethanesulfonyl fluoride, and Complete, and the collected cells were sonicated twice on ice for 30 s. Intact cells, cellular debris, and mitochondria were removed by centrifugation at 9000 × g for 10 min at 4 °C. Enzyme activities were measured as described above.

Isolation and Stimulation of Mouse Peritoneal Cells—Mouse peritoneal macrophages induced by thioglycollate (Difco) was prepared as described in detail previously (11). The cells were treated with 100 ng/ml LPS, 0.8 μM ODN1826, or 1 μg/ml poly(I:C), in the presence or absence of 100 nM DEX or 100 nM estradiol-17β for 16 h. After treatment, the cells were washed with an ice-cold buffer containing 20 mM Tris-HCl (pH 7.4) and 300 mM sucrose. Cell extracts were prepared by the same method as described for experiments using RAW264.7 cells, and the enzyme activity was measured.

After treatment with microbial components for 16 h, total RNA was collected using the Absolutely RNA RT-PCR miniprep kit. Likewise, at 4 h after intraperitoneal injection with 2 ml of 2% casein, peritoneal exudate neutrophils were harvested from the peritoneal cavity, and their total RNA was prepared.

Statistics—Data are presented as mean ± S.E. or S.D. p values less than 0.05 were considered statistically significant. All statistical calculations were performed using Prism 4 (GraphPad Software) and StatView-J, version 5.0 (Abacus Concepts, Berkeley, CA).

Mice—C57BL/6J mice were obtained from Clea Japan, Inc. (Tokyo, Japan). Mice were maintained in a light-dark cycle with light from 8:00 to 20:00 at 21 °C. Mice were fed with a standard laboratory diet and water *ad libitum*. All animal studies were conducted in accordance with the guidelines for Animal Research at The University of Tokyo and were approved by the University of Tokyo Ethics Committee for Animal Experiments.

RESULTS

Identification and Cloning of LysoPAFAT/LPCAT2—The mouse LysoPAFAT/LPCAT2 (mLysoPAFAT/LPCAT2) gene was identified based upon sequence homology with the previously reported LPCAT1 (27). The putative open reading frame of mLysoPAFAT/LPCAT2 encoded a 544-amino acid protein of 60.3 kDa, containing three putative transmembrane domains (36) and several conserved motifs found in members of the lysophospholipid acyltransferase family (27, 37). mLysoPAFAT/LPCAT2 contained putative EF-hand-like motifs (aa 374–494, E-value = 3e^*-10) predicted by a conserved domain data base (available on the World Wide Web at www.ncbi.nlm.nih.gov/Structure/cdd/cdd.shtml) (38) and showed 48.2% amino acid sequence homology to mouse LPCAT1. It exhibited 88.4% amino acid sequence homology to human LysoPAFAT/LPCAT2 (hLysoPAFAT/LPCAT2) (Fig. 1). The presence of the C-terminal sequence motif KK*XX* suggests that the protein is localized to the endoplasmic reticulum (ER) (39).

Tissue Distribution and Subcellular Localization of mLysoPAFAT/LPCAT2 mRNA—The tissue distribution of mLysoPAFAT/LPCAT2 was analyzed by quantitative PCR. We found the highest level of mLysoPAFAT/LPCAT2 expression in resident macrophages, casein-induced neutrophils, followed by skin, colon, spleen, and thioglycollate-induced macrophages (Fig. 2*A*). To facilitate immunocytochemical analysis of

FIGURE 1. **Amino acid sequence alignment of mouse and human LysoPAFAT/LPCAT2.** The predicted conserved lysophospholipid acyltransferase motifs (motifs 1–3) are *boxed*. The putative transmembrane domains are *underlined*. Amino acids conserved in both species are marked with *asterisks*. The ER localization sequence KKXX is present at the C terminus. The transmembrane motifs were determined using HMMTOP (available on the World Wide Web at www.enzim.hu/hmmtop/index.html).

mLysoPAFAT/LPCAT2, we constructed an expression vector encoding FLAG-tagged mLysoPAFAT/LPCAT2. It was transfected into CHO-K1, and the enzyme distribution was examined by confocal microscopy after 48 h. FLAG-mLysoPAFAT/LPCAT2 exhibited significant enzyme activities (Fig. 3, *A* and *B*). Cells were stained for ER-Golgi using $DiOC_6(3)$. The subcellular distribution pattern of FLAG-mLysoPAFAT/LPCAT2 was similar to that of $DiOC_6(3)$, suggesting that the enzyme is present mainly in the ER and Golgi (Fig. 2*B*).

Substrate Selectivity of mLysoPAFAT/LPCAT2—We next examined the acetyltransferase activity of mLysoPAFAT/LPCAT2 using a variety of 20 μM lysophospholipid acceptors and 100 μM [^{3}H]acetyl-CoA as a donor. mLysoPAFAT/LPCAT2 had detectable acetyltransferase activity toward LPC (Fig. 3*A*) and alkyl-LPC (Fig. 3*B*). The enzyme had a higher activity toward C16 lysophospholipids than C18 at the *sn*-1 moiety, which served as an acetyl acceptor (Fig. 3*B*). The acetyltransferase activity of mLysoPAFAT/LPCAT2 was linear for the first 40 min at 37 °C, and the enzyme exhibited calcium-dependent activity with a pH optimum around 7.4 (data not shown). To confirm whether the product of the acetyltransferase reaction is PAF, we first performed a competitive receptor binding assay using PAFR prepared from PAFR-transgenic mice (7, 34). Lipid extracts from the acetyltransferase reaction of mLysoPAFAT/LPCAT2 with lyso-PAF competed for binding of [^{3}H]WEB2086 to PAFR, indicating that the enzyme indeed produced PAF (supplemental Fig. 1). More definitively, the reaction product was identified by mass spectrometry (MS) using a 4000 Q-TRAP mass spectrometer (supplemental Fig. 2).

Human LysoPAFAT/LPCAT2 siRNA Decreases Lyso-PAF Acetyltransferase Activity—To investigate whether endogenous lyso-PAF acetyltransferase activity was decreased by transfection with an siRNA against hLysoPAFAT/LPCAT2, we transfected three hLysoPAFAT/LPCAT2 siRNAs (siRNA ID 140446, 140447, and 140448; Ambion) into HEK293 cells. We chose HEK293 cells, because the cells exhibit a high endogenous enzymic activity and high transfection efficiency (data not shown). All siRNAs decreased mRNA levels of hLysoPAFAT/LPCAT2 by 70–80% and lyso-PAF acetyltransferase activity by 50–60% (Fig. 3*C*). Control siRNA (silencer negative control 1; Ambion) had no apparent effect on either enzyme activity or mRNA expression. Thus, hLysoPAFAT/LPCAT2 appears to be the principal enzyme for PAF production in HEK293 cells.

LysoPAFAT/LPCAT2 Possesses LPC Acyltransferase Activity—Next, we examined the acyl-CoA selectivity of mLysoPAFAT/LPCAT2 using [^{3}H]lyso-PAF (C18) as an acceptor. At a high concentrations of acyl-CoAs (>20 μM), mLysoPAFAT/LPCAT2 showed both acetyltransferase and arachidonoyltransferase (acyltransferase) activities (Fig. 4). At a low concentration (<10 μM), arachidonoyl-CoA was a better substrate for LysoPAFAT/LPCAT2 than acetyl-CoA (Fig. 4). Medium chained fatty acyl-CoAs were poor substrates at both high and low concentrations of acyl-CoA (data not shown). These results suggest that mLysoPAFAT/LPCAT2 exhibits both lyso-PAF acetyltransferase and LPC acyltransferase activities. The apparent K_m values of the enzyme for acetyl-CoA and for arachidonoyl-CoA were 50.4 and 21.1 μM, respectively (Fig. 4).

Enzyme Activation by an Inflammatory Stimulus—Next, we investigated the activation of the enzyme by an inflammatory stimulus, such as LPS. To examine the response to LPS stimulation, mLysoPAFAT/LPCAT2 was transfected into the macrophage cell line, RAW264.7, which expresses the LPS receptor, Toll-like receptor 4 (TLR4), and cells were stimulated by LPS for 30 min in the presence or absence of the p38 mitogen-activated protein kinase inhibitor SB 203580 (Tocris Cookson). The acetyltransferase activity of mLysoPAFAT/LPCAT2 was

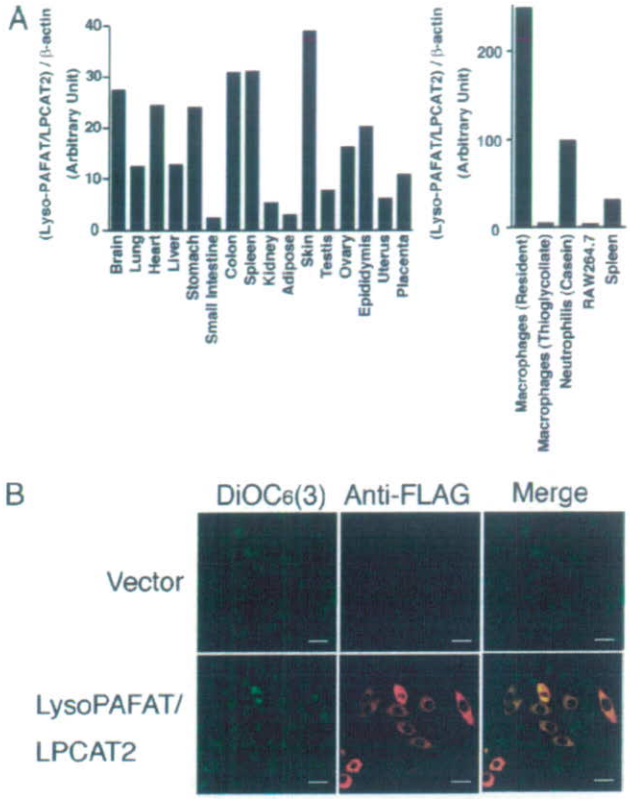

FIGURE 2. **Tissue distribution and subcellular localization of mLysoPAFAT/LPCAT2.** *A*, the expression levels of mLysoPAFAT/LPCAT2 and β-actin mRNA in 20 mouse tissues were analyzed by quantitative RT-PCR, and the levels of mLysoPAFAT/LPCAT2 mRNA were normalized to those of β-actin mRNA in each tissue. The highest level of mLysoPAFAT/LPCAT2 expression was observed in resident macrophages. *B*, CHO-K1 cells were transfected with FLAG-mLysoPAFAT/LPCAT2 and subjected to immunocytochemical analysis 48 h post-transfection. ER-Golgi and FLAG-mLysoPAFAT/LPCAT2 were visualized using $DiOC_6(3)$ (*green*) and the M5 anti-FLAG peptide antibody (*red*), respectively. The subcellular distribution pattern of FLAG-mLysoPAFAT/LPCAT2 was similar to that of $DiOC_6(3)$ (*Merge*), suggesting that the enzyme is present mainly in the ER and Golgi. $DiOC_6(3)$ is an ER-Golgi marker. The *scale bars* correspond to 20 μm. Results are representative of two independent experiments with similar results.

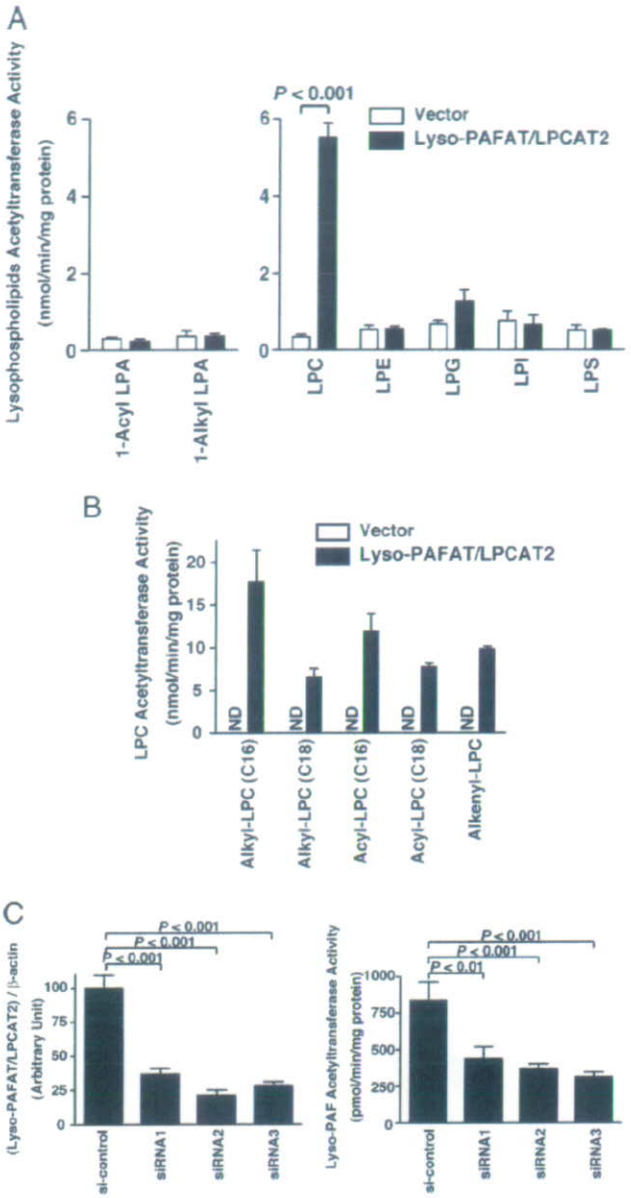

FIGURE 3. **Substrate selectivity of mLysoPAFAT/LPCAT2 and siRNA transfection with hLysoPAFAT/LPCAT2 siRNAs.** *A*, lysophospholipid acetyltransferase assays were performed by TLC with 20 μM lysophospholipid (1-acyl- and 1-alkyl-LPA, LPC, lysophosphatidylglycerol (*LPG*), lysophosphatidylethanolamine (*LPE*), lysophosphatidylinositol (*LPI*), or lysophosphatidylserine (*LPS*)) and 100 μM [^{3}H]acetyl-CoA in the presence of 1 μg of the microsomal fractions from vector-transfected (*open bars*) or mLysoPAFAT/LPCAT2-transfected (*closed bars*) cells. 1-*O*-Alkenyl-LPC (*heart*), LPI (*liver*), and LPS (*brain*) were from bovine tissues. Other lysophospholipids contained a palmitoyl group at the *sn*-1 position. *B*, several LPC (1-acyl-LPC C16, C18, 1-alkyl-LPC C16, C18, and 1-alkenyl-LPC) acetyltransferase activities were measured. mLysoPAFAT/LPCAT2 possessed lysophospholipid acetyltransferase activities toward 1-*O*-alkyl-LPC, 1-acyl-LPC, and 1-*O*-alkenyl-LPC. *ND*, not detectable. *C*, three hLysoPAFAT/LPCAT2 siRNAs and a control siRNA were transfected into HEK293 cells. After 48 h, mRNA levels (*left*) and lyso-PAF acetyltransferase activities (*right*) were measured, as described under "Experimental Procedures." Endogenous lyso-PAF acetyltransferase activity was reduced by each hLysoPAFAT/LPCAT2 siRNA. The data represent the mean ± S.D. of triplicate measurements. Statistical analyses were performed by analysis of variance and Tukey's multiple comparison test ($p < 0.01$). Two independent experiments were performed with similar results.

increased by LPS stimulation, but the effect was decreased in the presence of SB 203580; the acyltransferase activity of the enzyme was unchanged (Fig. 5). The endogenous lyso-PAF acyltransferase in RAW264.7 cells was activated by LPS, and this activation was blocked in the presence of SB 203580 (data not shown).

Induction of mLysoPAFAT/LPCAT2 mRNA—Next, we examined induction of mLysoPAFAT/LPCAT2 mRNA in response to long term treatment with Toll-like receptor agonists. Mouse thioglycollate-induced macrophages were treated with LPS (a TLR4 ligand), ODN1826 (a TLR9 ligand), or poly(I:C) (a TLR3 ligand) for 16 h in the presence or absence of DEX or estradiol-17β. As shown in Fig. 6*A*, the endogenous lyso-PAF acetyltransferase activity was enhanced 2.4- and 2.2-fold by LPS and ODN1826 treatment, respectively. Moreover, augmentation of the enzyme activity by LPS treatment was suppressed in the presence of DEX but not estradiol-17β. Similar results were obtained for the LPC acyltransferase activity (data not shown). The enzyme activation by ODN1826 also

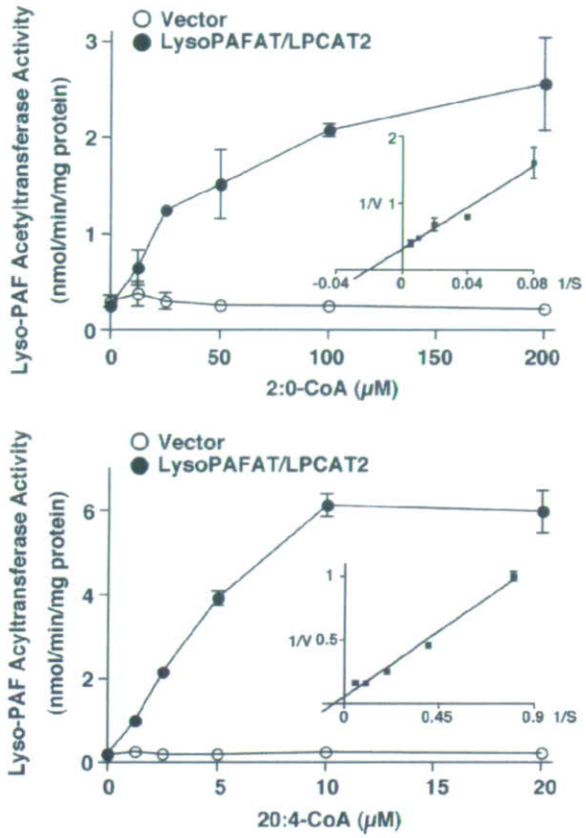

FIGURE 4. **Acetyltransferase and acyltransferase activities of mLysoPAFAT/LPCAT2.** Lyso-PAF acetyltransferase and acyltransferase assays were performed by TLC with the indicated concentrations of acetyl-CoA (2:0-CoA) and arachidonoyl-CoA (20:4-CoA) using 20 μM lyso-PAF. The *inset* shows a Lineweaver-Burk plot to calculate K_m values. The data represent the mean ± S.D. of triplicate measurements. The results are representative of two independent experiments with similar results.

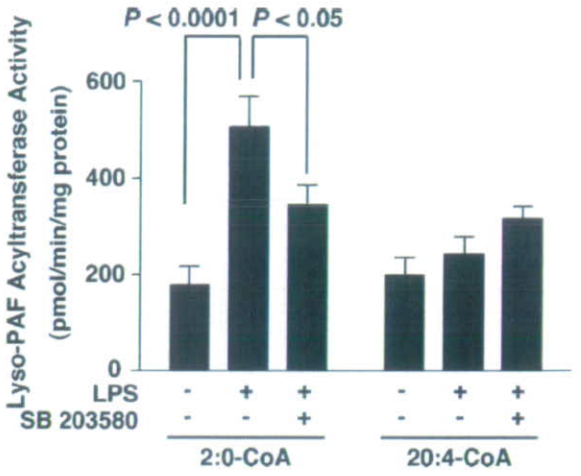

FIGURE 5. **Enzyme activation by an inflammatory stimulus.** RAW264.7 cells transfected with vector or mLysoPAFAT/LPCAT2 were stimulated with 100 ng/ml LPS in the presence or absence of SB 203580, and enzyme activity assays were performed subsequently. The difference between the activities obtained with vector and mLysoPAFAT/LPCAT2 corresponded to transfected enzyme activity. Endogenous acetyltransferase activities of nonstimulation, LPS stimulation, and LPS stimulation with SB203580 were 300.2, 469.0, and 259.4 pmol/min/mg protein, respectively. Endogenous acyltransferase activities were 604.0, 900.2, and 572.2 pmol/min/mg protein. Statistical analyses were performed by using analysis of variance with Fisher's projected least significant difference (PLSD) test ($p < 0.05$). The results are expressed as mean ± S.E. of three independent experiments, each performed in triplicate.

tended to be reduced by DEX. Poly(I:C) did not affect the lyso-PAF acetyltransferase activity in macrophages.

The mLysoPAFAT/LPCAT2 mRNA levels were increased 7.3- and 4.8-fold by LPS and ODN1826 treatment, respectively. Furthermore, induction of mLysoPAFAT/LPCAT2 by LPS was repressed by DEX treatment (Fig. 6*B*). ODN1826 also enhanced mLysoPAFAT/LPCAT2 levels, which tended to be reduced by DEX treatment. The expression level of mLysoPAFAT/LPCAT2 was not changed by poly(I:C) treatment, similar to the lack of effect on the enzyme activity (Fig. 6*A*). Induction of an IFNγ-inducible gene (IP-10) used as a positive control was observed by PCR after poly(I:C) stimulation under these conditions (data not shown).

DISCUSSION

This is the first report of isolation of a cDNA for LysoPAFAT/LPCAT2, a critically important enzyme in the biosynthesis of PAF. After long term treatments with a TLR4 or TLR9 agonist, the expression level of mLysoPAFAT/LPCAT2 mRNA was up-regulated, but not with a TLR3 agonist. Surprisingly, this enzyme catalyzed not only PAF biosynthesis (lyso-PAF acetyltransferase) but also generation of membrane glycerophospholipids (LPC acyltransferase), which are major membrane constituents and precursors of PAF. In the resting conditions, the enzyme prefers arachidonoyl-CoA to produce membrane lipids. However, under acute inflammatory stimulation by activating the TLR4, only the acetyltransferase activity of the enzyme was enhanced, and PAF production was augmented (Fig. 7).

Characterization of Lyso-PAF Acetyltransferase—mLysoPAFAT/LPCAT2 possessed lyso-PAF acetyltransferase activity but did not show 1-alkyl-LPA acetyltransferase activity, which catalyzes the first step of the *de novo* PAF biosynthesis pathway (Fig. 3, *A* and *B*) (2, 4). Using a heterologous overexpression system, we found that the enzyme was predominantly localized to the ER-Golgi complex (Fig. 2*B*). The exact localization of the endogenous protein in native cells remains to be determined. Additionally, LysoPAFAT/LPCAT2 possessed putative EF-hand-like motifs and showed calcium-dependent activity. These correlations remain to be further clarified. Using hLysoPAFAT/LPCAT2 siRNA transfection of HEK293 cells, both the mRNA and the enzyme activity of endogenous lyso-PAF acetyltransferase were significantly reduced (Fig. 3*C*), indicating that LysoPAFAT/LPCAT2 constitutes a major (50–80%) lyso-PAF acetyltransferase, in HEK293 cells. It is possible that other enzyme(s) are present also to catalyze PAF production in other tissues and cells.

LPC Acyltransferase Activity of LysoPAFAT/LPCAT2—mLysoPAFAT/LPCAT2 exhibited not only significant lyso-PAF acetyltransferase activity but also LPC acyltransferase activity (Fig. 4) *in vitro*, indicating that mLysoPAFAT/LPCAT2 can produce both PAF and PC. These data agree well with the previous studies showing that the lyso-PAF acetyltransferase activity in neutrophils was competed by long chain acyl-CoAs (40, 41). Recently, we and another group identified an LPC remod-

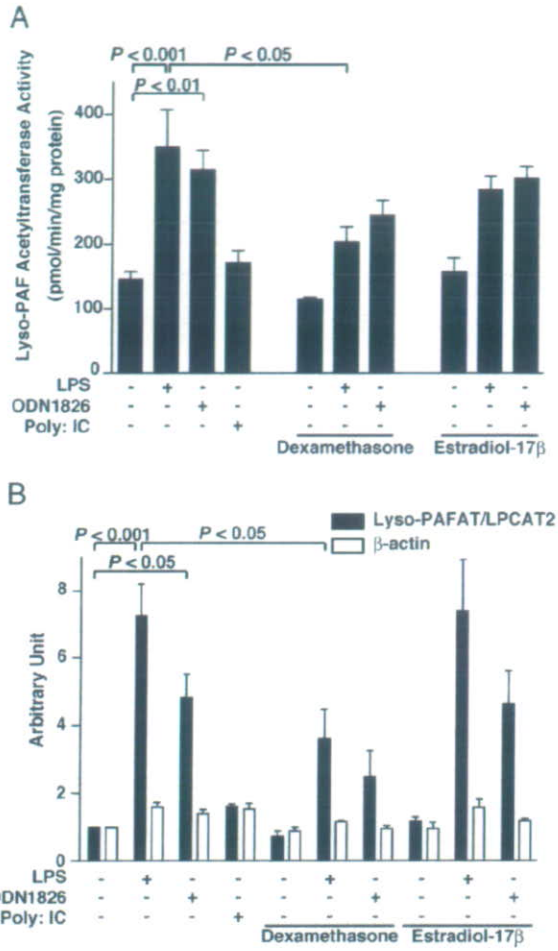

FIGURE 6. **Induction of LysoPAFAT/LPCAT2 by microbial components.** Thioglycollate-induced mouse macrophages were treated with 100 ng/ml LPS, 0.8 μM ODN1826, or 1 μg/ml poly(I:C) for 16 h in the presence or absence of 100 nM DEX or 100 nM estradiol-17β. Lyso-PAF acetyltransferase activity (*A*) and expression of mLysoPAFAT/LPCAT2 mRNA (*B*) were analyzed. The *open bars* indicate β-actin as a control. Statistical analyses were performed by analysis of variance and Tukey's multiple comparison test ($p < 0.05$). The results are expressed as mean ± S.E. of three independent experiments.

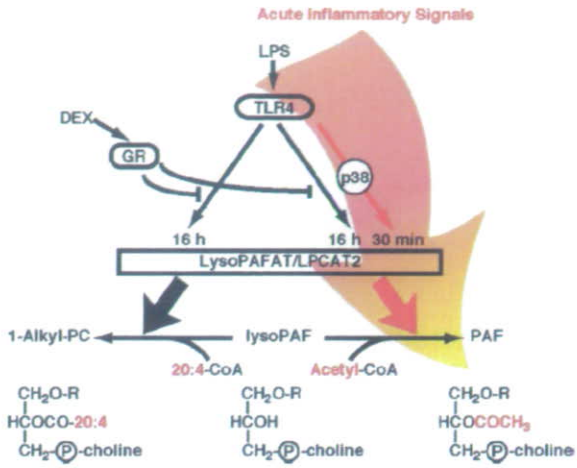

FIGURE 7. **Regulation of LysoPAFAT/LPCAT2 in mouse macrophages by inflammatory signals.** LysoPAFAT/LPCAT2 activity is increased by two distinct pathways in mouse macrophages. Although LysoPAFAT/LPCAT2 catalyzes both acetyltransferase and acyltransferase, only acetyltransferase activity was enhanced under acute inflammatory conditions. *GR*, glucocorticoid receptor; *p38*, p38 mitogen-activated protein kinase; *20:4-CoA*, arachidonoyl-CoA. See the first paragraph under "Discussion" for details.

eling enzyme, designated LPCAT1, which is highly expressed in lung (27, 28). In contrast, LysoPAFAT/LPCAT2 is predominantly expressed in inflammatory cells with modest expression in skin, brain, and colon. Because PC is biosynthesized in all cell types, a different class of LPCATs may exist in addition to LPCAT1 (27, 28) and LysoPAFAT/LPCAT2 (present study).

An Acute Inflammatory Response—Upon acute inflammatory stimulation by LPS, the acetyltransferase activity of mLysoPAFAT/LPCAT2 was enhanced (Fig. 5). Similar activation has been observed with endogenous lyso-PAF acetyltransferase in mouse peritoneal macrophages (11). Nixon *et al.* reported that lyso-PAF acetyltransferase in human neutrophils is directly activated by p38 mitogen-activated protein kinase (42). It is possible that LysoPAFAT/LPCAT2 is modified and activated by phosphorylation after LPS-stimulation. In contrast, the LPC acyltransferase activity of the enzyme was not changed by short term LPS stimulation (Fig. 5). The cellular signaling pathway mediating LysoPAFAT/LPCAT2 activation by LPS remains to be elucidated. In addition to putative conformational changes of the enzyme, both enzyme activities may be regulated by the ratio of two substrates (acetyl-CoA and arachidonoyl-CoA) in cells.

Induction of LysoPAFAT/LPCAT2 by Bacterial Components—Bacterial infections increase PAF production (1, 43, 44), and a TLR4 agonist (LPS) and a TLR9 agonist (ODN1826) induced the enzyme activity and mRNA levels of LysoPAFAT/LPCAT2. LPS activates both MyD88 (myeloid differentiation primary response gene 88) and TRIF (Toll/interleukin-1 receptor domain-containing adaptor inducing interferon-β) adaptor protein (45–47). These results suggest that LysoPAFAT/LPCAT2 expression is regulated in a MyD88-dependent manner in the innate immune system, because TLR9 and TLR3 mediate MyD88- and TRIF-dependent pathways, respectively (45, 48, 49). Induction of mLysoPAFAT/LPCAT2 was attenuated by DEX treatment (Fig. 6). Ogawa *et al.* (50) reported that glucocorticoid receptor signaling represses LPS-mediated up-regulation of a large set of related inflammatory response genes, such as cyclooxygenase-2 and interleukin-6. Furthermore, DEX inhibits LPS-induced plasma PAF release (51). It will be important to determine the transcriptional regulation and cis-elements of LysoPAFAT/LPCAT2 in future studies.

LPS-induced accumulation of LysoPAFAT/LPCAT2 increases acyltransferase activity in addition to the acetyltransferase activity. The biological significance of up-regulation of the acyltransferase activity may be related to the fact that under long term LPS stimulation, cytosolic and secretory phospholipase A_2 are activated, leading to increased release of free fatty acids and lysophospholipids from PC (52, 53). Lysophospholipids are toxic to cells because of their detergent effects. Alternatively, active membrane remodeling is required during inflammatory responses, such as phagocytosis or chemotaxis. LysoPAFAT/LPCAT2 may play an important role in the regulation of lysophospholipid and PAF levels and in the storage of PC as PAF precursor membrane glycerophospholipids.

Conclusion—We have isolated a new enzyme that catalyzes PAF production and membrane biogenesis (LysoPAFAT/LPCAT2). Further studies are needed to elucidate the roles of mLysoPAFAT/LPCAT2 *in vivo* and to determine its potential as a novel therapeutic target for various diseases involving PAF biosynthesis. It will be important to characterize both acetyltransferase and acyltransferase activities of the enzyme, including identification of binding sites for each substrate (acetyl-CoA and arachidonoyl-CoA) and differential regulation of individual enzyme activity. Molecular cloning and characterization of this first LysoPAFAT/LPCAT2 will enable us to better understand the biochemical mechanisms underlying PAF and phospholipid biosynthesis in inflammatory cells.

Acknowledgments—We are grateful to Drs. A. Yamashita (Teikyo University), T. Yokomizo, (Kyushu University), K. Kume (Kumamoto University), M. Nakamura, T. Takahashi, Y. Kita, and Y. Iizuka (University of Tokyo) and all members of our laboratory for valuable suggestions and F. Hamano (University of Tokyo) for technical assistance. We also thank Dr. J. Miyazaki for supplying pCXN2.

REFERENCES

1. Ishii, S., and Shimizu, T. (2000) *Prog. Lipid Res.* **39,** 41–82
2. Prescott, S. M., Zimmerman, G. A., and McIntyre, T. M. (1990) *J. Biol. Chem.* **265,** 17381–17384
3. Ishii, S., Kuwaki, T., Nagase, T., Maki, K., Tashiro, F., Sunaga, S., Cao, W. H., Kume, K., Fukuchi, Y., Ikuta, K., Miyazaki, J., Kumada, M., and Shimizu, T. (1998) *J. Exp. Med.* **187,** 1779–1788
4. Snyder, F. (1995) *Biochim. Biophys. Acta* **1254,** 231–249
5. Serhan, C. N., Haeggstrom, J. Z., and Leslie, C. C. (1996) *FASEB J.* **10,** 1147–1158
6. Kihara, Y., Ishii, S., Kita, Y., Toda, A., Shimada, A., and Shimizu, T. (2005) *J. Exp. Med.* **202,** 853–863
7. Shindou, H., Ishii, S., Uozumi, N., and Shimizu, T. (2000) *Biochem. Biophys. Res. Commun.* **271,** 812–817
8. Doebber, T. W., and Wu, M. S. (1987) *Proc. Natl. Acad. Sci. U. S. A.* **84,** 7557–7561
9. Lee, T., Lenihan, D. J., Malone, B., Roddy, L. L., and Wasserman, S. I. (1984) *J. Biol. Chem.* **259,** 5526–5530
10. Owen, J. S., Baker, P. R., O'Flaherty, J. T., Thomas, M. J., Samuel, M. P., Wooten, R. E., and Wykle, R. L. (2005) *Biochim. Biophys. Acta* **1733,** 120–129
11. Shindou, H., Ishii, S., Yamamoto, M., Takeda, K., Akira, S., and Shimizu, T. (2005) *J. Immunol.* **175,** 1177–1183
12. Uozumi, N., Kume, K., Nagase, T., Nakatani, N., Ishii, S., Tashiro, F., Komagata, Y., Maki, K., Ikuta, K., Ouchi, Y., Miyazaki, J., and Shimizu, T. (1997) *Nature* **390,** 618–622
13. Shimizu, T., Ohto, T., and Kita, Y. (2006) *IUBMB Life* **58,** 328–333
14. Wykle, R. L., Malone, B., and Snyder, F. (1980) *J. Biol. Chem.* **255,** 10256–10260
15. Arai, H. (2002) *Prostaglandins Other Lipid Mediat.* **68,** 83–94
16. Venable, M. E., Olson, S. C., Nieto, M. L., and Wykle, R. L. (1993) *J. Biol. Chem.* **268,** 7965–7975
17. Honda, Z., Nakamura, M., Miki, I., Minami, M., Watanabe, T., Seyama, Y., Okado, H., Toh, H., Ito, K., Miyamoto, T., and Shimizu, T. (1991) *Nature* **349,** 342–346
18. Hattori, M., Adachi, H., Tsujimoto, M., Arai, H., and Inoue, K. (1994) *Nature* **370,** 216–218
19. Tjoelker, L. W., Wilder, C., Eberhardt, C., Stafforini, D. M., Dietsch, G., Schimpf, B., Hooper, S., Le Trong, H., Cousens, L. S., Zimmerman, G. A., Yamadat, Y., McIntyre, T. M., Prescott, S. M., and Gray, P. W. (1995) *Nature* **374,** 549–553
20. Kume, K., Waga, I., and Shimizu, T. (1997) *Anal. Biochem.* **246,** 118–122
21. Gomez-Cambronero, J., Velasco, S., Sanchez-Crespo, M., Vivanco, F., and Mato, J. M. (1986) *Biochem. J.* **237,** 439–445
22. Fragopoulou, E., Iatrou, C., and Demopoulos, C. A. (2005) *Mediators Inflamm.* **2005,** 263–272
23. Kennedy, E. P. (1961) *Fed. Proc.* **20,** 934–940
24. Lands, W. E. M. (1960) *J. Biol. Chem.* **235,** 2233–2237
25. Lands, W. E. M., and Merkl, I. (1963) *J. Biol. Chem.* **238,** 898–904
26. Merkl, I., and Lands, W. E. M. (1963) *J. Biol. Chem.* **238,** 905–906
27. Nakanishi, H., Shindou, H., Hishikawa, D., Harayama, T., Ogasawara, R., Suwabe, A., Taguchi, R., and Shimizu, T. (2006) *J. Biol. Chem.* **281,** 20140–20147
28. Chen, X., Hyatt, B. A., Mucenski, M. L., Mason, R. J., and Shannon, J. M. (2006) *Proc. Natl. Acad. Sci. U. S. A.* **103,** 11724–11729
29. Li, D., Yu, L., Wu, H., Shan, Y., Guo, J., Dang, Y., Wei, Y., and Zhao, S. (2003) *J. Hum. Genet.* **48,** 438–442
30. Niwa, H., Yamamura, K., and Miyazaki, J. (1991) *Gene (Amst.)* **108,** 193–199
31. Bradford, M. M. (1976) *Anal. Biochem.* **72,** 248–254
32. Bligh, E. G., and Dyer, W. J. (1959) *Can. J. Biochem. Physiol.* **37,** 911–917
33. Aoki, Y., Nakamura, M., Kodama, H., Matsumoto, T., Shimizu, T., and Noma, M. (1995) *J. Immunol. Methods* **186,** 225–231
34. Ishii, S., Nagase, T., Tashiro, F., Ikuta, K., Sato, S., Waga, I., Kume, K., Miyazaki, J., and Shimizu, T. (1997) *EMBO J.* **16,** 133–142
35. Houjou, T., Yamatani, K., Nakanishi, H., Imagawa, M., Shimizu, T., and Taguchi, R. (2004) *Rapid Commun. Mass Spectrom.* **18,** 3123–3130
36. Tusnady, G. E., and Simon, I. (2001) *Bioinformatics* **17,** 849–850
37. Lewin, T. M., Wang, P., and Coleman, R. A. (1999) *Biochemistry* **38,** 5764–5771
38. Marchler-Bauer, A., Anderson, J. B., Cherukuri, P. F., DeWeese-Scott, C., Geer, L. Y., Gwadz, M., He, S., Hurwitz, D. I., Jackson, J. D., Ke, Z., Lanczycki, C. J., Liebert, C. A., Liu, C., Lu, F., Marchler, G. H., Mullokandov, M., Shoemaker, B. A., Simonyan, V., Song, J. S., Thiessen, P. A., Yamashita, R. A., Yin, J. J., Zhang, D., and Bryant, S. H. (2005) *Nucleic Acids Res.* **33,** D192–196
39. Shikano, S., and Li, M. (2003) *Proc. Natl. Acad. Sci. U. S. A.* **100,** 5783–5788
40. Reinhold, S. L., Zimmerman, G. A., Prescott, S. M., and McIntyre, T. M. (1989) *J. Biol. Chem.* **264,** 21652–21659
41. Remy, E., Lenoir, G., Houben, A., Vandesteene, C., and Remacle, J. (1989) *Biochim. Biophys. Acta* **1005,** 87–92
42. Nixon, A. B., O'Flaherty, J. T., Salyer, J. K., and Wykle, R. L. (1999) *J. Biol. Chem.* **274,** 5469–5473
43. Benigni, A., Boccardo, P., Noris, M., Remuzzi, G., and Siegler, R. L. (1992) *Lancet* **339,** 835–836
44. Smith, J. M., Jones, F., Ciol, M. A., Jelacic, S., Boster, D. R., Watkins, S. L., Williams, G. D., Tarr, P. I., and Henderson, W. R., Jr. (2002) *Pediatr. Nephrol.* **17,** 1047–1052
45. Akira, S., Uematsu, S., and Takeuchi, O. (2006) *Cell* **124,** 783–801
46. Kawai, T., Takeuchi, O., Fujita, T., Inoue, J., Muhlradt, P. F., Sato, S., Hoshino, K., and Akira, S. (2001) *J. Immunol.* **167,** 5887–5894
47. Yamamoto, M., Sato, S., Hemmi, H., Hoshino, K., Kaisho, T., Sanjo, H., Takeuchi, O., Sugiyama, M., Okabe, M., Takeda, K., and Akira, S. (2003) *Science* **301,** 640–643
48. Hemmi, H., Takeuchi, O., Kawai, T., Kaisho, T., Sato, S., Sanjo, H., Matsumoto, M., Hoshino, K., Wagner, H., Takeda, K., and Akira, S. (2000) *Nature* **408,** 740–745
49. Alexopoulou, L., Holt, A. C., Medzhitov, R., and Flavell, R. A. (2001) *Nature* **413,** 732–738
50. Ogawa, S., Lozach, J., Benner, C., Pascual, G., Tangirala, R. K., Westin, S., Hoffmann, A., Subramaniam, S., David, M., Rosenfeld, M. G., and Glass, C. K. (2005) *Cell* **122,** 707–721
51. Han, S. J., Choi, J. H., Ko, H. M., Yang, H. W., Choi, I. W., Lee, H. K., Lee, O. H., and Im, S. Y. (1999) *Eur. J. Immunol.* **29,** 1334–1341
52. Shinohara, H., Balboa, M. A., Johnson, C. A., Balsinde, J., and Dennis, E. A. (1999) *J. Biol. Chem.* **274,** 12263–12268
53. Balsinde, J., Balboa, M. A., Yedgar, S., and Dennis, E. A. (2000) *J. Biol. Chem.* **275,** 4783–4786

Journal of Neurochemistry, 2007, **102**, 1658–1668 doi:10.1111/j.1471-4159.2007.04796.x

Reduced pain behaviors and extracellular signal-related protein kinase activation in primary sensory neurons by peripheral tissue injury in mice lacking platelet-activating factor receptor

Makoto Tsuda,* Satoshi Ishii,†‡ Takahiro Masuda,* Shigeo Hasegawa,* Koji Nakamura,* Kenichiro Nagata,* Tomohiro Yamashita,* Hidemasa Furue,§ Hidetoshi Tozaki-Saitoh,* Megumu Yoshimura,§ Schuichi Koizumi,¶ Takao Shimizu† and Kazuhide Inoue*

**Department of Molecular and System Pharmacology, Graduate School of Pharmaceutical Sciences, Kyushu University, Maidashi, Higashi-ku, Fukuoka, Japan*

†Department of Biochemistry and Molecular Biology, Faculty of Medicine, The University of Tokyo, Hongo, Bunkyo-ku, Tokyo, Japan

‡Precursory Research for Embryonic Science and Technology (PRESTO) of Japan Science and Technology Agency, Hongo, Bunkyo-ku, Tokyo, Japan

§Department of Integrative Physiology, Graduate School of Medical Sciences, Kyushu University, Maidashi, Higashi-ku, Fukuoka, Japan

¶Department of Pharmacology, Interdisciplinary Graduate School of Medicine and Engineering, University of Yamanashi, Shimokato, Chuo, Yamanashi, Japan

Abstract

Peripheral tissue injury causes the release of various mediators from damaged and inflammatory cells, which in turn activates and sensitizes primary sensory neurons and thereby produces persistent pain. The present study investigated the role of platelet-activating factor (PAF), a phospholipid mediator, in pain signaling using mice lacking PAF receptor (*pafr–/–* mice). Here we show that *pafr–/–* mice displayed almost normal responses to thermal and mechanical stimuli but exhibit attenuated persistent pain behaviors resulting from tissue injury by locally injecting formalin at the periphery as well as capsaicin pain and visceral inflammatory pain without any alteration in cytoarchitectural or neurochemical properties in dorsal root ganglion (DRG) neurons and a defect in motor function. However, *pafr–/–* mice showed no alterations in spinal pain behaviors caused by intrathecally administering agonists for *N*-methyl-D-aspartate (NMDA) and neurokinin$_1$ receptors. A PAFR agonist evoked an intracellular Ca^{2+} response predominantly in capsaicin-sensitive DRG neurons, an effect was not observed in *pafr–/–* mice. By contrast, the PAFR agonist did not affect C- or Aδ-evoked excitatory postsynaptic currents in substantia gelatinosa neurons in the dorsal horn. Interestingly, mice lacking PAFR showed reduced phosphorylation of extracellular signal-related protein kinase (ERK), an important kinase for the sensitization of primary sensory neurons, in their DRG neurons after formalin injection. Furthermore, U0126, a specific inhibitor of the ERK pathway suppressed the persistent pain by formalin. Thus, PAFR may play an important role in both persistent pain and the sensitization of primary sensory neurons after tissue injury.

Keywords: mitogen-activated protein kinase, platelet-activating factor receptor, primary afferent sensory neurons, tissue injury pain.

J. Neurochem. (2007) **102**, 1658–1668.

Received 5 January, 2007; revised manuscript received 27 April, 2007; accepted 30 May, 2007.

Address correspondence and reprint requests to Kazuhide Inoue, PhD, Department of Molecular and System Pharmacology, Graduate School of Pharmaceutical Sciences, Kyushu University, 3-1-1 Maidashi, Higashi-ku, Fukuoka 812-8582, Japan. E-mail: inoue@phar.kyushu-u.ac.jp

Abbreviations used: $[Ca^{2+}]_i$, intracellular Ca^{2+}; EPSC, excitatory postsynaptic current; CV, conduction velocity; ERK, extracellular signal-related protein kinase; fura-2AM, fura-2 acetoxymethylester; mcPAF, methylcarbamyl PAF; MEK, mitogen-activated protein kinase kinase; PAF, platelet-activating factor; PAFR, PAF receptor; septide, [pGlu^6, L-Pro^9]substance P (6–11); SG, substantia gelatinosa; TRPV1, transient receptor potential vanilloid type 1.

Primary afferent sensory neurons transmit sensory information received at the periphery to dorsal horn neurons in the spinal cord. Once peripheral tissue has been damaged, the damaged cells or surrounding inflammatory cells release a variety of mediators. Some stimulate directly nociceptors and elicit pain responses, and the others develop sensitization of primary sensory neurons to physical and chemical stimuli by activating intracellular protein kinases or by changing the gene expression and thereby result in enabling easier activation of the pain pathway. These events act together to create a persistent pain state (Julius and Basbaum 2001; Mayer *et al.* 2006).

Platelet-activating factor (PAF, 1-*O*-alkyl-2-acetyl-*sn*-glycero-3-phosphocholine) is a phospholipid mediator that regulates the functions of a variety of cells not only in the peripheral tissues but also in the nervous system (Ishii and Shimizu 2000; Prescott *et al.* 2000). The biological activities of PAF are elicited by activating its receptor, PAF receptor (PAFR), which belongs to the superfamily of G protein-coupled receptors (Honda *et al.* 1991; Ishii *et al.* 1998). Several studies have investigated the role of the PAF/PAFR system in modulating pain signaling. Local injection of PAF into the rat hindpaw increases the sensitivity to noxious stimulation (Bonnet *et al.* 1981; Belanger *et al.* 1987; Dallob *et al.* 1987). The lack of the response by injection of lyso-PAF (a structurally related, biologically inactive form) appears to involve PAFR (Belanger *et al.* 1987). Administering PAF into human skin also produces a hypersensitive state (Archer *et al.* 1984; Basran *et al.* 1984). These studies suggest that PAF might exaggerate pain. PAF is produced by various kinds of cells including keratinocytes (Alappatt *et al.* 2000) and inflammatory cells (Montrucchio *et al.* 2000), and the level of PAF is increased in inflamed tissue (Noguchi *et al.* 1989; Kihara *et al.* 2005; Doi *et al.* 2006). However, much less is known about the role of endogenous PAF/PAFR system in nociception. Although a recent behavioral study investigated this by means of pharmacological tools, such as BN52021, an antagonist for PAFR, the compound is not specific for PAFR since it was demonstrated to have antagonistic effects on glycine- and GABA-gated chloride channels (Kondratskaya *et al.* 2002; Ivic *et al.* 2003; Huang *et al.* 2004). In addition, some other PAFR antagonists have been reported to have an inverse agonistic effect (Dupre *et al.* 2001), an inhibitory effect on the activity of intracellular PAF acetylhydrolase, an inactivating enzyme of PAF (Adachi *et al.* 1997) or an antagonistic effect on histamine receptor (Merlos *et al.* 1997). Thus, these pharmacological problems of PAFR antagonists have been a major barrier to revealing the precise role of the endogenous PAF/PAFR system in pain signaling. Therefore, in the present study, we used mice that lack PAFR (*pafr*−/−) by targeted disruption of the gene (Ishii *et al.* 1998) and investigated the behavioral phenotype in a range of pain tests. Here we demonstrate that the PAF/PAFR system is important for persistent pain behaviors caused by tissue injury as well as capsaicin and visceral pain, and that the lack of PAFR results in a reduction of tissue injury-induced extracellular signal-related protein kinase (ERK) activation in primary afferent sensory neurons, an important kinase in sensitization (Dai *et al.* 2002; Obata and Noguchi 2004; Zhuang *et al.* 2004).

Materials and methods

Animals

All of the animals have been used in accordance with the guidelines of National Institute of Health Sciences, Kyushu University and The University of Tokyo. *pafr*−/− mice were established using a gene-targeting strategy (Ishii *et al.* 1998). Male *pafr*−/− mice and their wild-type littermates (9- to 11-week-old) used here have been backcrossed for 6–10 generations onto a C57BL/6 N genetic background. Within each experimental group, the sex ratio and the backcross generation were equal, and the age did not differ significantly. Male Wistar rats were also used some experiments.

Pain behavior studies

Noxious heat-evoked tail and hindpaw withdrawal responses were detected by the application of radiant heat (Ugo Basile, Italy) to the tail and the plantar surface of hindpaw, respectively (Tsuda *et al.* 1999a, 2000). The intensity of the heat stimulus was adjusted to 30 or 50 V, and the latency of the paw withdrawal response (s) was measured. The sensitivity to mechanical stimulus was assessed using von Frey filaments (0.02–2.0 g) (Stoelting, Wood Dale, IL, USA), and the mechanical stimulus producing the 50% paw withdrawal threshold was determined (Tsuda *et al.* 2003). In the tests of formalin- and capsaicin-induced pain, mice were injected intraplantarly with formalin (5%, 20 μL for mice; 2%, 100 μL for rats) and capsaicin (1.6 μg), respectively, and then the duration of the licking and biting responses to the injected hindpaw was recorded at 5 min intervals for 60 min after the injection (formalin pain) and for a period of 5 min (capsaicin pain) (Tsuda *et al.* 1999b). For the measurement of hindpaw swelling by formalin, the weights of the left (formalin) and right (phosphate-buffered saline) hind feet amputated at the ankle were measured 60 min after the injection of formalin. In the chemical visceral pain test, mice were injected i.p. with acetic acid (0.8%), and the number of abdominal writhes was counted for 5 min starting from 5 min after the injection. In the tests for pain responses at the spinal level, mice were injected intrathecally with NMDA (0.2 μg/5 μL) or with [pGlu^6, L-Pro^9]substance P (6–11) (septide; 10 μg/5 μL) (Sigma, St Louis, MO, USA), and the total duration of scratching, biting, and licking behaviors was recorded for 5 min (Sakurada *et al.* 1998). Motor coordination was assessed using the rotarod performance test (Tsuda *et al.* 1999b). For administering U0126, a mitogen-activated protein kinase kinase (MEK) inhibitor, under isoflurane anesthesia, a 32 gauge catheter (ReCathCo, Allison Park, PA, USA) was inserted through the atlanto-occipital membrane, and the tip of the catheter was positioned near the L5 dorsal root ganglion (L5 DRG). Rats were injected with U0126 (20 nmol/10 μL; Tocris, Bristol, UK) through the catheter 10 min before the injection of formalin into the hindpaw.

Intracellular calcium ($[Ca^{2+}]_i$) imaging

Acute dissociated DRGs from Wistar rats, wild-type and *pafr*−/− mice were used (Tsuda *et al.* 1999a, 2000). Cells were plated on poly-L-lysine-coated glass coverslips with silicon rubber walls (Flexiperm, W.C. GmbH, Germany). The increase in $[Ca^{2+}]_i$ in single cells was measured by the fura-2 technique (Koizumi *et al.* 1994). The cells were incubated with 5 μmol/L fura-2 acetoxymethylester (fura-2AM; Dojindo, Kumamoto, Japan) for 30 min in balanced salt solution (composition in mmol/L: NaCl 150, KCl 5, $CaCl_2$ 1.2, $MgCl_2$ 1.2, D-glucose 10 and HEPES 25; pH 7.4). Then, the cells were washed with balanced salt solution and mounted on an inverted fluorescence microscope (TMD-300, Nikon, Japan) equipped with a xenon-lamp and band-pass filters of 340 nm wavelength and 360 nm wavelength. The emission fluorescence was measured at 510 nm. Image data were processed by a Ca^{2+}-analysing system (Furusawa Lab. Appliance Co., Japan). KCl (75 mmol/L, 5 s), methylcarbamyl PAF (mcPAF: 1 μmol/L, 10 s) and capsaicin (1 μmol/L) were applied to the DRG neurons.

Patch-clamp recordings from substantial gelatinosa neurons of the spinal dorsal horn

We used spinal cord slice preparations from rats in order to precisely distinguish the effect of mcPAF between Aδ- and C-mediated excitatory post-synaptic currents (EPSCs) in SG neurons. A 600-μm thick transverse slice of the fifth lumber (L5) spinal cord with the L5 dorsal root from Wistar rat was cut using a vibratome (Yoshimura and Jessell 1989). The slice was placed on nylon mesh in the recording chamber, and then perfused at a rate of 10–15 mL min−1 with Krebs solution (composition in mmol/L: NaCl 117, KCl 3.6, $CaCl_2$ 2.5, $MgCl_2$ 1.2, NaH_2PO_4 1.2, $NaHCO_3$ 25 and glucose 11) saturated with 95% O_2 – 5% CO_2, and maintained at 36 ± 1°C. Blind whole-cell voltage-clamp recordings were made from SG neurons (Yoshimura and Nishi 1993). The patch pipettes were filled with a solution (composition in mmol/L: potassium gluconate 136, KCl 5, $CaCl_2$ 0.5, $MgCl_2$ 2, EGTA 5, HEPES 5 and MgATP 5). The tip resistance of the patch pipette was 8–12 MΩ. In the voltage-clamp mode, the holding potentials (V_H) were −70 mV. Stimuli (duration, 100 μs) to elicit EPSCs were given to the dorsal root at a frequency of 0.2 Hz via a suction electrode. The Aδ- or C-afferent-mediated responses evoked by the dorsal root stimulation were distinguished on the basis of the conduction velocity (CV) of the afferent fibers (C, < 0.8 m/s; Aδ, 2–11 m/s) and stimulus threshold (C, >300 μA; Aδ, 40–200 μA), as previously described (Yoshimura and Jessell 1989). The CV was calculated from the latency of the synaptic responses from a stimulus artifact and the length of the dorsal root. The Aδ-afferent-mediated EPSCs were considered to be monosynaptic in nature when the latency remained constant and there was no failure during repetitive stimulation at 20 Hz for 1 s. The C-afferent-mediated EPSCs were considered to be monosynaptic when failures did not occur during stimulation at 2 Hz for 10 s (Nakatsuka *et al.* 1999, 2000). Signals were acquired with a patch clamp amplifier (Axopatch 200B, Molecular Devices, Union City, CA, USA). The data were digitized with an analog-to-digital converter (Digidata 1321 A, Molecular Devices) and analyzed using a special software package (Clampfit version 10.0). mcPAF was applied by perfusion via a three-way stopcock without any change in the perfusion rate or the temperature.

Immunohistochemistry

The anesthetized mice were perfused transcardially with 20 mL of phosphate-buffered saline followed by 50 mL of ice-cold 4% paraformaldehyde 3 min after intraplantar injection with 5% formalin. The L4/5 segments of the DRG were removed, post-fixed in the same fixative, and placed in 30% sucrose for 24 h at 4°C. L4/5 DRG or L5 spinal cord sections (30 μm) attached on a slide-glass were incubated in a blocking solution (3% normal goat serum) and then incubated with anti-phospho-ERK (1 : 200, Cell Signaling, Beverly, MA, USA), anti-TRPV1 (1 : 200, Oncogene, San Diego, CA, USA) or anti-NeuN (1:200, Chemicon, Temecula, CA, USA) for 48 h at 4°C. After washing, tissue sections were incubated with anti-rabbit IgG conjugated Alexa Fluor™ 488 (1 : 1000, Molecular Probes, Eugene, OR, USA) for 3 h at 22–24°C. The sections were analyzed using a LSM510 Imaging System (Zeiss, Oberkochen, Germany). Three to four sections of the L4 DRG from each genotypes (n = 4) were selected randomly. The number of phospho-ERK-positive neuronal profiles that showed distinctive phospho-ERK labeling compared with background labeling in DRG sections was counted and was divided by the total number of neurons, and the percentage of immunoreactive neuron profiles was obtained. For the size-frequency analyses, measurement of the cross-sectional areas of TRPV1 immunoreactive-positive neurons (wild type: 418 cells, *pafr*−/−: 330 cells) was made by using an LSM Image Browser (Zeiss) and only neurons with clearly visible nuclei were used for the quantification.

Statistical analyses

Analysis of the time-course of the duration of licking and biting response was performed by two factors (group × times) repeated measures analysis of variance (ANOVA). The other results were evaluated using the Student's t-test or Mann-Whitney U-test.

Results

Acute pain behaviors in *pafr*−/− mice

To examine the sensitivities to acute physiological pain, the withdrawal responses from the noxious range of radiant heat and mechanical stimuli by von Frey filaments were measured in both wild-type and *pafr*−/− mice. In the tail-flick test, the latencies to flick their tail from heat at both 30 and 50 V were not different between wild-type and *pafr*−/− mice (Fig. 1a). The latency to withdraw their hindpaw from heat was not altered at 50 V, but was slightly increased at 30 V in *pafr*−/− mice ($p < 0.05$, Fig. 1b). In a test of mechanical pain, *pafr*−/− mice were indistinguishable from wild-type mice in the paw withdrawal threshold (Fig. 1c).

We subsequently tested the effect of PAFR ablation on chemical-induced cutaneous pain behaviors evoked by intraplantar injection of capsaicin, an activator of transient receptor potential vanilloid type 1 (TRPV1) channel which is expressed in nociceptors (Caterina and Julius 2001). Wild-type mice exhibited intense licking and biting responses to the injected hindpaw, but *pafr*−/− mice spent

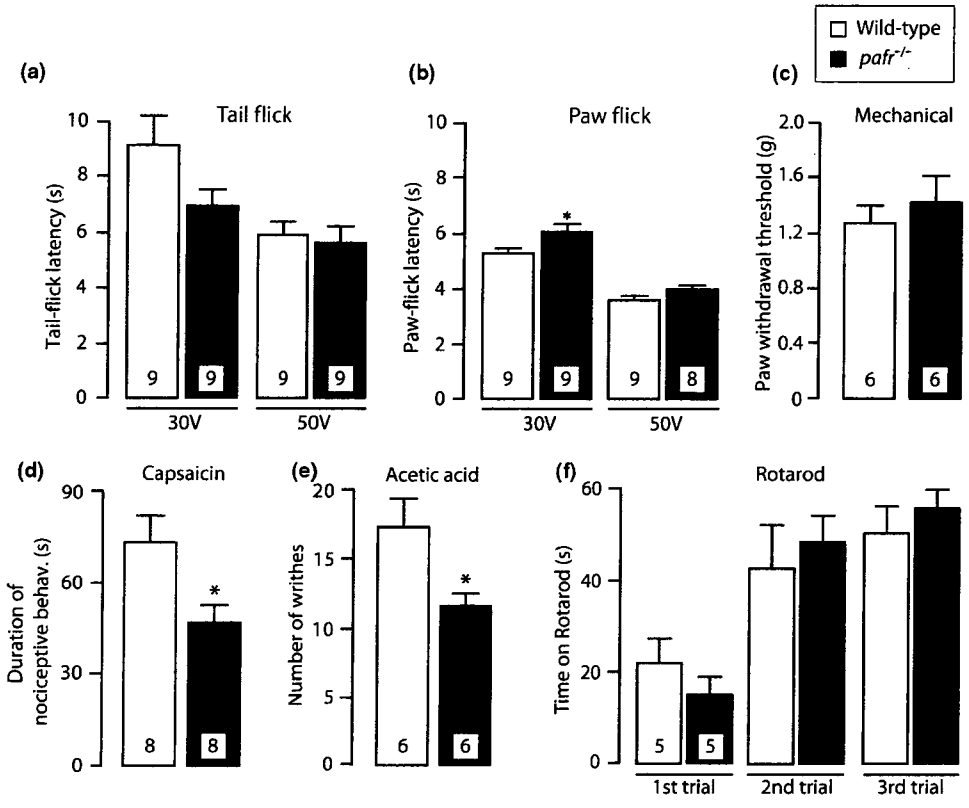

Fig. 1 Acute thermal and mechanical pain and chemical-induced pain in *pafr*–/– mice. (a and b) Tail-flick and paw-flick tests, respectively. Values represent the latency (s) to tail or paw flick from the heat source. *$p < 0.05$ versus wild-type. (c) Mechanical pain test. Values indicate the threshold (g) to elicit paw withdrawal behavior in response to noxious mechanical stimuli. (d) Capsaicin test. Capsaicin (1.6 μg/20 μL) was injected intraplantarly into the hindpaw. Values represent the duration of licking and biting responses measured for 5 min after the injection. *$p < 0.05$ versus wild-type. (e) Visceral pain in response to acetic acid (0.8%). Values represent the number of abdominal stretches (writhes). *$p < 0.05$ versus wild-type. (f) Rotarod performance test. Values represent the duration (s) that mice remain on the rotating rod measured three times. All data are presented as mean ± SEM of 5–9 mice.

significantly less time licking and biting ($p < 0.05$, Fig. 1d). We also found that abdominal writhing behavior in response to intraperioneal injection with acetic acid, a model of chemical-induced visceral inflammatory pain, was significantly reduced in *pafr*–/– mice ($p < 0.05$, Fig. 1e). A reduction in pain behaviors is occasionally misinterpreted as a result of non-specific motor dysfunction, but the rotarod performance test demonstrated no significant difference in either the time on the rotarod at the first trial or an increase in the time on the rotarod throughout the trials between the two genotypes (Fig. 1f).

Impaired tissue injury-induced pain behavior in *pafr*–/– mice

To determine the role of PAFR in tissue injury-induced acute and persistent pain, we assessed the pain response following the injection of formalin into the hindpaw. In wild-type mice, injection of formalin elicited biphasic biting and licking behaviors: the first phase started immediately after the injection and lasted for 5 min, and the second phase lasted for 60 min (Fig. 2a). The pattern of biphasic behaviors was not altered in *pafr*–/– mice, but the magnitude was significantly reduced ($F_{1,12} = 2.703$, $p < 0.01$) (Fig. 2a). A significant difference was observed during 0–5 min (first phase, $p < 0.01$) and during 25–35 min ($p < 0.05$) after the injection (Fig. 2a). *pafr*–/– mice displayed a significant reduction to 35% of the pain response during 10–35 min in the second phase after the injection of formalin ($p < 0.05$, Fig. 2b). The second phase is related to the hyperexcitability of primary afferent neurons in response to inflammation, but the degree of formalin-induced swelling of the injected hindpaw, as indicated by an increase in the weight of the hindpaw 60 min after the injection, was not significantly different between the two genotypes (Fig. 2c). Our data show that PAFR has a crucial role in the modulation of injury-induced pain.

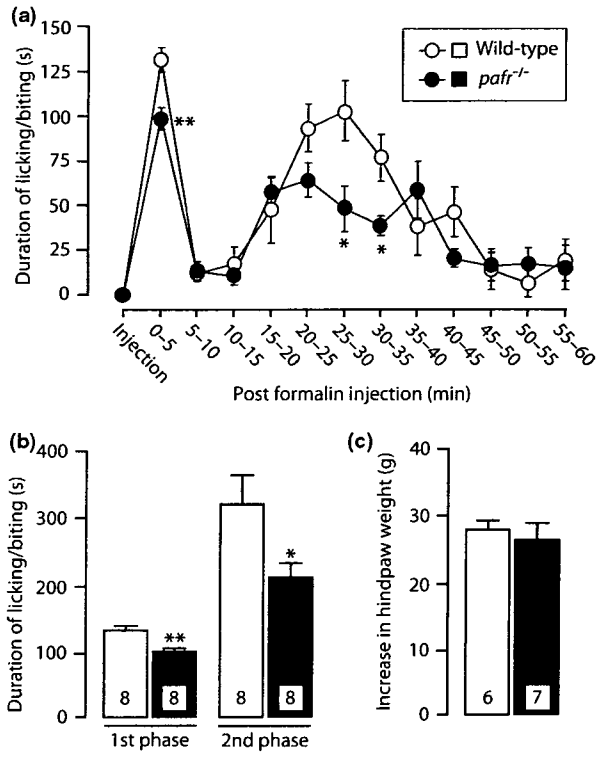

Fig. 2 Impaired pain behavior following tissue injury by formalin in *pafr*–/– mice. (a and b) Formalin pain. Mice were injected intraplantarly with formalin (5%). Values represent the duration (s) of licking and biting responses for each 5-min interval (a), from 0 to 5 min (first phase) and for 10–35 min (second phase) (b), and the change in the weight of the hindpaw 60 min after the injection of formalin (5%) or PBS (c). $^{*}p < 0.05$, $^{**}p < 0.01$ versus wild-type. All data are presented as mean ± SEM of 6–8 mice.

Histological characterization of dorsal root ganglion neurons in *pafr*–/– mice

To investigate whether the lack of PAFR alters cytoarchitectural and neurochemical properties in DRG neurons, we measured the cross-sectional areas of total and TRPV1-positive (TRPV1+) DRG neurons with clearly visible nuclei and analyze their size frequency distributions. As shown in Fig. 3a, no alterations were observed in the size frequency and the mean somal area of total DRG neurons between wild-type (446.4 μm^2 ± 31.3) and *pafr*–/– mice (468.1 μm^2 ± 16.1). In wild-type mice, TRPV1 immunoreactivity was observed predominantly in small-sized neurons (mean somal area: 203.9 μm^2 ± 1.3) and the percentage of TRPV1+ neurons was 34.3% of total DRG neurons (Fig. 3b). The mean somal area (197.0 μm^2 ± 2.4) and percentage (35.0%) in the DRG of *pafr*–/– mice was similar to those of wild-type mice. Furthermore, TRPV1 immunoreactivities in the dorsal horn of both wild-type and *pafr*–/– mice were localized in the superficial lamina (Fig. 3c). In addition, there was no clear difference in the

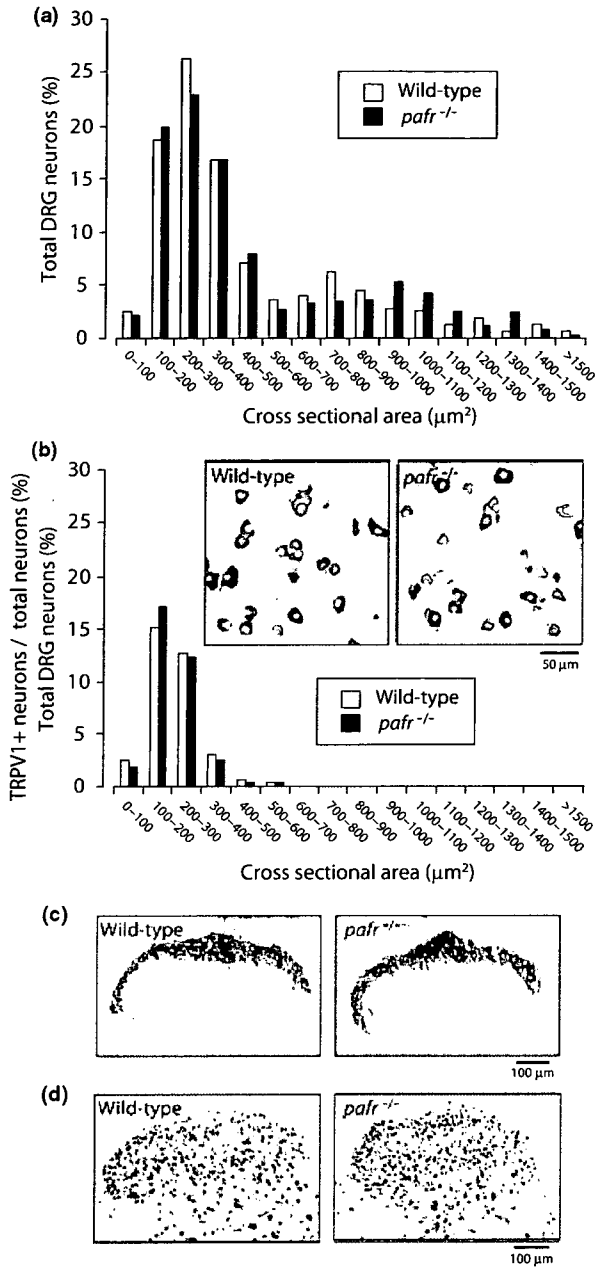

Fig. 3 Cytoarchitectural and neurochemical properties in dorsal root ganglion (DRG) neurons in *pafr*–/– mice. (a and b) Size-frequency histogram illustrating the distribution of the cross-sectional areas of total (a) and TRPV1-positive (b) DRG neurons of wild-type and *pafr*–/– mice. Inset photographs in the panel (b) showing TRPV1 immunoreactivity in the DRG of both strains. Scale bar: 50 μm. (c and d) Immunoreactivities of TRPV1 (c) and NeuN (d) in the dorsal horn of wild-type and *pafr*–/– mice. Scale bar: 100 μm.

immunoreactivity or localization of the neuronal marker NeuN in the dorsal horn between both strains (Fig. 3d). These observations suggest that wild-type and *pafr*–/–

mice have similar cytoarchitectural and neurochemical properties in DRG neurons.

PAF receptor agonist-evoked intracellular Ca^{2+} responses in dorsal root ganglion neurons

Activating PAFR causes Ca^{2+} mobilization through stimulating the G-protein/phospholipase C/IP_3 pathway (Ishii and Shimizu 2000; Honda *et al.* 2002). To examine whether functional PAFR are expressed, we monitored changes in the level of intracellular Ca^{2+} ($[Ca^{2+}]_i$) following an application of methylcarbamyl PAF (mcPAF), a PAFR agonist, in individual DRG neurons. We first applied 75 mmol/L KCl to distinguish neuronal cells. In the DRG neuronal cells (n = 193 cells), mcPAF (1 μmol/L) produced an increase in the 340/360 emission ratio for fura-2 (n = 21 cells) (Fig. 4), indicating that activating PAFR caused an increase in $[Ca^{2+}]_i$ in a subset of DRG neurons. Interestingly, most of the mcPAF-sensitive DRG neurons also responded to capsaicin (1 μmol/L) (n = 18). Moreover, in capsaicin-sensitive DRG neurons from wild-type mice, mcPAF also produced an increase in $[Ca^{2+}]_i$ (5 of 37 cells tested), which was not observed in *pafr*−/− mice (0 of 41 cells tested). These results indicate the presence of functional PAFR in DRG neurons that appear to be nociceptors.

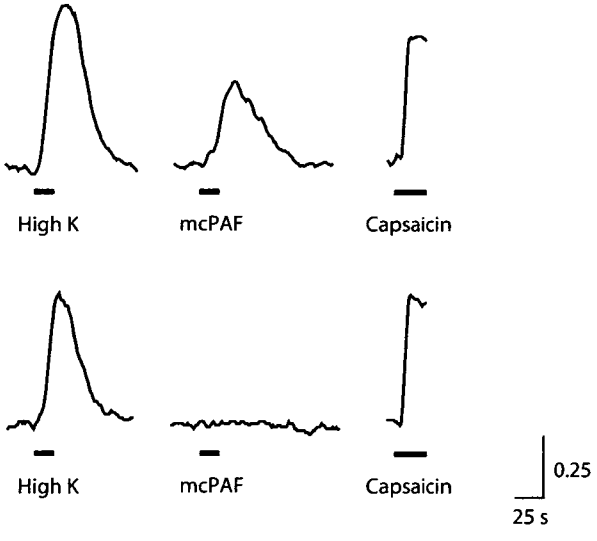

Fig. 4 Ca^{2+} response in individual primary afferent sensory neurons by PAF receptor (PAFR) agonist. Intracellular Ca^{2+} imaging analysis using the Ca^{2+}-sensitive fluorescent dye fura-2 was performed. The traces show KCl (75 mmol/L, 5 s)-evoked a transient increase in the 340/360 emission ratio for fura-2 in acute dissociated dorsal root ganglion (DRG) neurons (n = 193 cells). In 193 DRG neurons, 21 neurons showed an increase in the ratio when applying methylcarbamyl PAF (mcPAF: 1 μmol/L, 10 s) (upper). The other cells (n = 172) did not respond (lower). Most of the mcPAF-responsive DRG neurons (n = 18) also showed an increase in the ratio by capsaicin (1 μmol/L).

Roles of PAF receptor on synaptic transmission in spinal dorsal horn neurons and spinal pain behaviors

Activation of primary afferent sensory neurons causes the release of neurotransmitters in the dorsal horn. To examine whether PAFR has a role in modulating synaptic transmission in the dorsal horn, we recorded dorsal root stimulation-evoked EPSCs in substantia gelatinosa (SG) neurons where primary afferent terminals terminate, using spinal cord slices with attached dorsal roots. Stimulation of the dorsal root always evoked EPSCs with monosynaptic Aδ- and C-afferent properties (Fig. 5a). The CVs of Aδ- and C-afferent fibers for those recordings were 6.4 ± 1.1 and 0.6 ± 0.1 m/s (Fig. 5a), within the range of Aδ- and C-afferent fiber CVs, respectively (Yoshimura and Jessell 1989). The bath application of mcPAF (30 and 60 μmol/L) for 1 min did not alter the amplitude of the Aδ- and C-evoked EPSCs in SG neurons (Fig. 5b).

Glutamate and substance P are major neurotransmitters released from primary sensory neurons in the dorsal horn and activate NMDA receptors and tachykinin NK_1 receptors on dorsal horn neurons, respectively (Nichols *et al.* 1999; South *et al.* 2003). We thus examined whether PAFR deletion

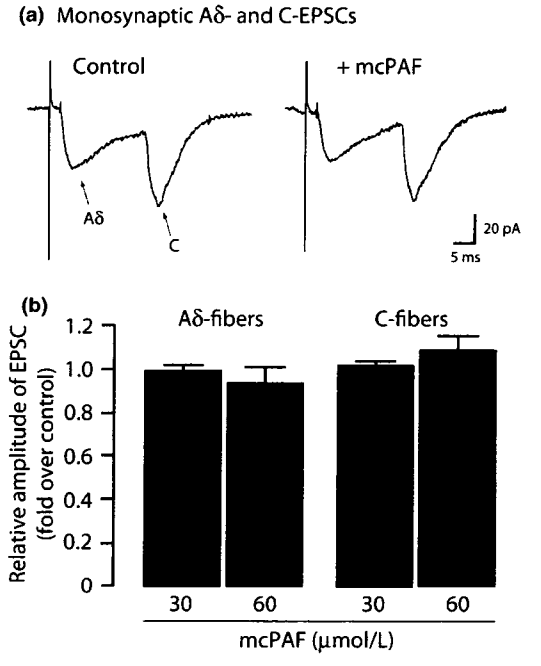

Fig. 5 Effect of PAF receptor (PAFR) agonist on glutamatergic excitatory post-synaptic currents (EPSCs) in substantia gelatinosa (SG) neurons by stimulating the dorsal roots. (a) Traces of monosynaptic Aδ- and C-fibers before (control) and just after the treatment with methylcarbamyl PAF (mcPAF: 30 and 60 μmol/L, 1 min) (+mcPAF). (b) Peak amplitudes of monosynaptic Aδ- and C-fiber-evoked EPSCs under the action of mcPAF, relative to those in the control. V_H = −70 mV. The data are presented as mean ± SEM of 3–11 SG neurons.

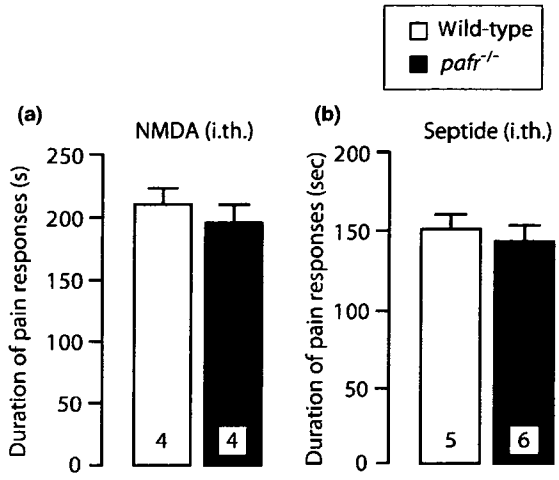

Fig. 6 Spinal pain evoked by intrathecal administration of agonists for NMDA and NK_1 receptors (a and b). Mice were injected intrathecally with NMDA (0.2 μg/5 μL) (a) or septide (10 μg/5 μL) (b). Values indicate the duration (s) of pain responses (licking, biting, and scratching) for 5 min after the injection. All data are presented as mean ± SEM of 4–6 mice.

affected the NMDA and NK_1 receptor-mediated pain responses. Administering intrathecally NMDA (0.2 μg/5 μL) and septide (10 μg/5 μL), an agonist for NK_1, to wild-type mice both produced biting, licking, and scratching behaviors (Fig. 6a and b). The duration of pain responses was altered in *pafr*−/− mice neither by NMDA nor by septide (Fig. 6a and b). These results indicate a minor role of PAFR in pain processing in the spinal dorsal horn under a normal condition.

Reduced ERK activation in DRG neurons following tissue injury in *pafr*−/− mice

As noted above, *pafr*−/− mice displayed a reduction in the persistent phase of tissue injury pain. We investigated the role of PAFR in the activation of ERK in primary sensory neurons, which is an important kinase in sensitization and therefore in persistent pain (Dai *et al.* 2002; Obata and Noguchi 2004; Zhuang *et al.* 2004). Activated ERK was detected by immunofluorescence labeling with an antibody for recognizing phosphorylated ERK (phospho-ERK). In the DRG from wild-type mice after intraplantar injection of formalin, phospho-ERK-positive neurons were observed in 8% of total DRG neurons (82/947 cells, Fig. 7a, c). By contrast, the numbers of phospho-ERK-positive neurons in the DRG from *pafr*−/− mice after formalin injection were significantly fewer, and the percentage of cells positive to phospho-ERK was decreased to 3% of total cells ($p < 0.05$) (39/1204 cells, Fig. 7b, c). Our data suggest that PAFR is required for the ERK activation in primary afferent sensory neurons following tissue injury.

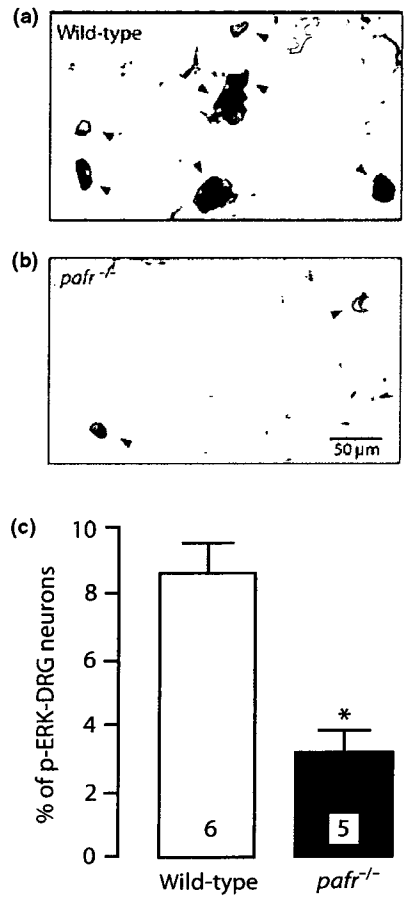

Fig. 7 Reduced extracellular signal-related protein kinase (ERK) activation in primary sensory neurons by tissue injury in *pafr*−/− mice. (a and b) Photographs of phospho-ERK-immunostained L4/5 DRG section of wild-type (a) and *pafr*−/− mice (b) 3 min after injection of formalin (5%). Scale bar: 50 μm. (c) The percentage of phospho-ERK-positive neurons (arrowheads in a and b) in the total neurons counted. $^*p < 0.05$ versus wild-type. The data are presented as mean ± SEM of 5–6 mice.

To determine the functional relevance of ERK activation to the tissue injury-induced pain behavior, we injected the selective MEK inhibitor U0126 into rats through a catheter whose tip was positioned near the L5 DRG and examined its effect on the formalin-induced pain behaviors. In this experiment, we used rats in order to apply U0126 preferentially to the L5 DRG rather than to the L5 spinal cord. The pattern of biphasic behaviors was almost similar between both groups (Fig. 8a). U0126 did not alter the duration of the first phase (Fig. 8b), but the duration of the second phase of the pain response was significantly suppressed by the pretreatment with U0126 ($p < 0.05$, Fig. 8b) as compared with vehicle-treated rats. These results indicate that ERK activation is important in the expression of the persistent phase of formalin-induced pain behavior.

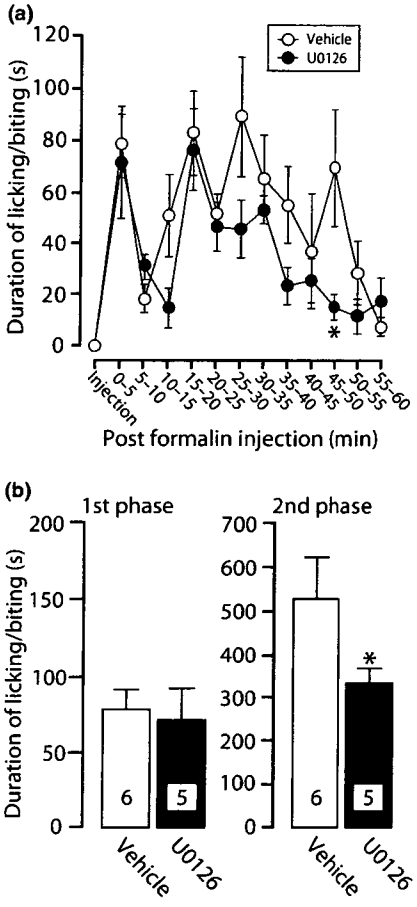

Fig. 8 Reduced persistent phase of formalin-induced pain behavior by pretreatment with U0126. (a) Values represent the duration (s) of licking and biting responses for each 5-min interval (a). (b) The sums of the durations of the formalin-induced biting and licking response during first phase (0–5 min; left) and second phase (10–60 min, right) after 2% formalin injection. The mitogen-activated protein kinase kinase (MEK) inhibitor U0126 (20 nmol/10 μL) was injected through a catheter whose tip was positioned near the L5 DRG 10 min before the formalin injection. $^*p < 0.05$ versus vehicle-treated group. Each point and column represents the mean ± SEM of 5–6 rats.

Discussion

To reveal the precise role of PAFR in pain signaling, we employed a series of pain tests using mice lacking PAFR and found that *pafr*−/− mice exhibited impaired persistent pain behaviors resulting from tissue injury by locally injecting formalin at the periphery without any non-specific motor dysfunction. *pafr*−/− mice also showed a reduction of the acute pain behaviors that are evident in formalin injury-induced pain, capsaicin-induced cutaneous pain and acetic acid-induced visceral pain. By contrast, the behavioral responses to brief noxious thermal and mechanical stimulation in *pafr*−/− mice were comparable to those of wild-type littermates. These results thus indicate that *pafr*−/− mice do not show alterations in all forms of pain responses but rather exhibit aberrant phenotypes in specialized pain states.

It appeared that the acute pain behaviors that were reduced in *pafr*−/− mice were related to nociceptor stimulation. Capsaicin stimulates nociceptors via the activation of TRPV1 channels (Caterina and Julius 2001), and the acute phase of formalin pain is also related to the direct stimulation of nociceptors by formalin (Tjolsen *et al.* 1992; McCall *et al.* 1996; Puig and Sorkin 1996). However, *pafr*−/− mice showed no alteration in their responses to brief noxious stimulation. Although one possibility is that the lack of PAFR may alter cytoarchitectural and neurochemical properties of DRG neurons, we did not observe any changes in the size-frequency distribution and the mean cell area of either total or TRPV1-positive DRG neurons between wild-type and *pafr*−/− mice. One of the differences in these pain tests was the duration of nociceptors stimulation. Indeed, excitation of C-fibers is observed at least for 2–3 min after the injection of formalin (McCall *et al.* 1996; Puig and Sorkin 1996), which is much longer than that from applying noxious thermal stimuli (less than 10 s; Fig. 1). Thus, the PAF/PAFR system may become active in response to a relatively prolonged stimulation of nociceptors. Although the reduced pain behaviors in the first phase of formalin pain in *pafr*−/− mice conflicts with the data of a previous work showing that PAFR antagonists did not suppress the first phase (Teather *et al.* 2002), this might be explained by the pharmacological non-specificity of PAFR antagonists (Kondratskaya *et al.* 2002) and by the difference in the experimental procedures (the indicator of the pain response and the concentration of formalin).

Our Ca^{2+} imaging study showing that a PAFR agonist produced a Ca^{2+} response in capsaicin-sensitive DRG neurons, presumably through stimulating the G-protein/phospholipase C/IP_3 pathway (Ishii and Shimizu 2000; Honda *et al.* 2002), suggests the presence of functional PAFR in nociceptors. This notion is supported by previous data that PAFR mRNA is detected in the DRG (Morita *et al.* 2004) and that a PAFR agonist induces gene expression in primary sensory neurons (Nakasaki *et al.* 1999). However, we observed no alterations in the afferent-evoked EPSCs in SG neurons by PAFR agonist nor in spinal pain behaviors between wild-type and *pafr*−/− mice, suggesting that PAFR has a minor role in excitatory synaptic transmission in SG neurons. This is apparently in contrast to previous data showing that intrathecal administration of PAF produces hypersensitivity to innocuous mechanical stimuli (tactile allodynia), which is mediated by glutamate receptors in the spinal cord (Morita *et al.* 2004). It is conceivable that activating PAFR may modulate synaptic transmission in dorsal horn neurons other than SG neurons, which could be involved in tactile allodynia caused by intrathecal administration of PAF. At the periphery, local injection of PAFR

agonist has been demonstrated not to produce spontaneous pain behaviors (e.g., licking or biting response) (Wheeler-Aceto *et al.* 1990) but rather to enhance the sensitivities to noxious stimuli (Bonnet *et al.* 1981; Belanger *et al.* 1987; Dallob *et al.* 1987). PAF is released from keratinocytes (Alappatt *et al.* 2000) and inflammatory cells, such as neutrophils, eosinophils, monocytes/macrophages, and vascular endothelial cells (Montrucchio *et al.* 2000). The level of PAF is indeed increased in inflamed peripheral tissue (Noguchi *et al.* 1989; Doi *et al.* 2006). These results together suggest that a lack of the PAF/PAFR system of primary afferent sensory neurons may be responsible for the reduced pain behaviors, especially by tissue injury, in *pafr*−/− mice.

An important finding in the present study is that PAFR plays a role in the activation of ERK in the primary sensory neurons as well as in persistent pain behaviors following peripheral tissue injury. ERK has recently received attention as an intracellular event generating sensitization of primary sensory neurons to peripheral inputs (Dai *et al.* 2002; Obata and Noguchi 2004; Zhuang *et al.* 2004). The persistent phase of formalin pain that was attenuated in *pafr*−/− mice (Fig. 2a, b) has been considered to be associated in part with the hyperexcitability of primary sensory neurons at the inflamed site induced by formalin (McCall *et al.* 1996; Puig and Sorkin 1996; Pitcher and Henry 2002). We also found that the formalin-induced persistent pain was suppressed by the MEK inhibitor U0126 administered near the L5 DRG where is a very long distance away from the L5 spinal cord. These data suggest that the impairment in the persistent pain behaviors in *pafr*−/− mice may be associated with the reduced tissue injury-induced ERK activation in cell bodies of primary sensory neurons in the DRG, although we can not exclude a possible involvement of ERK in dorsal horn neurons (Ji *et al.* 1999) or central afferent terminals in the suppressing effect of U0126. Additionally, an alteration of the gene expression by ERK (Obata and Noguchi 2004) suggests the possibility that PAFR may also play a role in more long-term adaptive changes following tissue injury.

The reduction in the proportion of phosphorylated ERK-positive DRG neurons (about 5%) in *pafr*−/− mice was slightly lower than that of mcPAF-responded DRG neurons that had been acutely dissociated from the DRG (about 10 % of DRG neurons tested). Considering the fact that L4/5 DRG neurons projects their fibers not only to the plantar area of the hindpaw but also to other targets, such as the viscera, muscle and skin of other areas (Thornton *et al.* 2005), a subpopulation of PAFR-expressing DRG neurons may project to the plantar surface and be associated with ERK activation in response to tissue injury by formalin.

The mechanisms underlying the ERK activation in sensory neurons by PAFR remain unclear, but several possibilities are considered. Our present data showing that lacking PAFR reduced ERK activation in DRG neurons that occurred shortly after formalin injection suggest the possibility that activating PAFR by PAF presumably released at the periphery in response to tissue injury may increase signals that lead to ERK activation in cell bodies of DRG neurons such as the action potentials (Fields *et al.* 1997; Dai *et al.* 2002) or the TRPV1 channel activity (Dai *et al.* 2002) at the periphery. Alternatively, since the PAF level is increased in inflamed tissue (Noguchi *et al.* 1989; Kihara *et al.* 2005; Doi *et al.* 2006). PAF (or coordinated with other chemical mediators) may produce a direct activation of ERK at peripheral nerve endings, which has been implicated in causing peripheral sensitization (Dai *et al.* 2002), and may secondary activate ERK in cell bodies of DRG neurons. Indeed, a subset of DRG neurons has been reported to activate ERK by stimulating G protein-coupled receptors (Aley *et al.* 2001), and PAFR stimulation causes the phosphorylation of ERK in various cells (Ishii and Shimizu 2000; Honda *et al.* 2002).

Tissue-damaging stimuli generate a complex cascade of transmitters and modulators at the periphery, which in turn develop tissue injury-induced persistent pain (Julius and Basbaum 2001). The present findings obtained from mice lacking PAFR have now provided evidence that PAFR signaling activated by endogenous PAF may be an important event in producing persistent pain and ERK activation in primary sensory neurons after peripheral tissue injury.

Acknowledgements

This work was supported by grants from the Ministry of Education, Culture, Sports, Science and Technology of Japan (to MT, KI).

References

Adachi T., Aoki J., Manya H., Asou H., Arai H. and Inoue K. (1997) PAF analogues capable of inhibiting PAF acetylhydrolase activity suppress migration of isolated rat cerebellar granule cells. *Neurosci. Lett.* **235**, 133–136.

Alappatt C., Johnson C. A., Clay K. L. and Travers J. B. (2000) Acute keratinocyte damage stimulates platelet-activating factor production. *Arch. Dermatol. Res.* **292**, 256–259.

Aley K. O., Martin A., McMahon T., Mok J., Levine J. D. and Messing R. O. (2001) Nociceptor sensitization by extracellular signal-regulated kinases. *J. Neurosci.* **21**, 6933–6939.

Archer C. B., Page C. P., Paul W., Morley J. and MacDonald D. M. (1984) Inflammatory characteristics of platelet activating factor (PAF-acether) in human skin. *Br. J. Dermatol.* **110**, 45–50.

Basran G. S., Page C. P., Paul W. and Morley J. (1984) Platelet-activating factor: a possible mediator of the dual response to allergen? *Clin. Allergy* **14**, 75–79.

Belanger P., Maycock A., Guindon Y. *et al.* (1987) L-656,224 (7-chloro-2-[(4-methoxyphenyl)methyl]-3- methyl-5-propyl-4-benzofuranol): a novel, selective, orally active 5-lipoxygenase inhibitor. *Can. J. Physiol. Pharmacol.* **65**, 2441–2448.

Bonnet J., Loiseau A. M., Orvoen M. and Bessin P. (1981) Platelet-activating factor acether (PAF-acether) involvement in acute inflammatory and pain processes. *Agents Actions* **11**, 559–562.

Caterina M. J. and Julius D. (2001) The vanilloid receptor: a molecular gateway to the pain pathway. *Annu. Rev. Neurosci.* **24**, 487–517.

Dai Y., Iwata K., Fukuoka T., Kondo E., Tokunaga A., Yamanaka H., Tachibana T., Liu Y. and Noguchi K. (2002) Phosphorylation of extracellular signal-regulated kinase in primary afferent neurons by noxious stimuli and its involvement in peripheral sensitization. *J. Neurosci.* **22**, 7737–7745.

Dallob A., Guindon Y. and Goldenberg M. M. (1987) Pharmacological evidence for a role of lipoxygenase products in platelet-activating factor (PAF)-induced hyperalgesia. *Biochem. Pharmacol.* **36**, 3201–3204.

Doi K., Okamoto K., Negishi K. *et al.* (2006) Attenuation of folic acid-induced renal inflammatory injury in platelet-activating factor receptor-deficient mice. *Am. J. Pathol.* **168**, 1413–1424.

Dupre D. J., Le Gouill C., Rola-Pleszczynski M. and Stankova J. (2001) Inverse agonist activity of selected ligands of platelet-activating factor receptor. *J. Pharmacol. Exp. Ther.* **299**, 358–365.

Fields R. D., Eshete F., Stevens B. and Itoh K. (1997) Action potential-dependent regulation of gene expression: temporal specificity in Ca^{2+}, cAMP-responsive element binding proteins, and mitogen-activated protein kinase signaling. *J. Neurosci.* **17**, 7252–7266.

Honda Z., Nakamura M., Miki I. *et al.* (1991) Cloning by functional expression of platelet-activating factor receptor from guinea-pig lung. *Nature* **349**, 342–346.

Honda Z., Ishii S. and Shimizu T. (2002) Platelet-activating factor receptor. *J. Biochem. (Tokyo)* **131**, 773–779.

Huang S. H., Duke R. K., Chebib M., Sasaki K., Wada K. and Johnston G. A. (2004) Ginkgolides, diterpene trilactones of *Ginkgo biloba*, as antagonists at recombinant $\alpha_1\beta_2\gamma_{2\,L}$ $GABA_A$ receptors. *Eur. J. Pharmacol.* **494**, 131–138.

Ishii S. and Shimizu T. (2000) Platelet-activating factor (PAF) receptor and genetically engineered PAF receptor mutant mice. *Prog. Lipid Res.* **39**, 41–82.

Ishii S., Kuwaki T., Nagase T. *et al.* (1998) Impaired anaphylactic responses with intact sensitivity to endotoxin in mice lacking a platelet-activating factor receptor. *J. Exp. Med.* **187**, 1779–1788.

Ivic L., Sands T. T., Fishkin N., Nakanishi K., Kriegstein A. R. and Stromgaard K. (2003) Terpene trilactones from Ginkgo biloba are antagonists of cortical glycine and $GABA_A$ receptors. *J. Biol. Chem.* **278**, 49279–49285.

Ji R. R., Baba H., Brenner G. J. and Woolf C. J. (1999) Nociceptive-specific activation of ERK in spinal neurons contributes to pain hypersensitivity. *Nat. Neurosci.* **2**, 1114–1119.

Julius D. and Basbaum A. I. (2001) Molecular mechanisms of nociception. *Nature* **413**, 203–210.

Kihara Y., Ishii S., Kita Y., Toda A., Shimada A. and Shimizu T. (2005) Dual phase regulation of experimental allergic encephalomyelitis by platelet-activating factor. *J. Exp. Med.* **202**, 853–863.

Koizumi S., Watano T., Nakazawa K. and Inoue K. (1994) Potentiation by adenosine of ATP-evoked dopamine release via a pertussis toxin-sensitive mechanism in rat phaeochromocytoma PC12 cells. *Br. J. Pharmacol.* **112**, 992–997.

Kondratskaya E. L., Lishko P. V., Chatterjee S. S. and Krishtal O. A. (2002) BN52021, a platelet activating factor antagonist, is a selective blocker of glycine-gated chloride channel. *Neurochem. Int.* **40**, 647–653.

Mayer R. A., Ringkamp M., Campbell J. N. and McMahon S. B. (2006) *Peripheral Mechanisms of Cutaneous Nociception*, 5th Edn, pp 3–34. Elsevier, Churchill-Livingstone.

McCall W. D., Tanner K. D. and Levine J. D. (1996) Formalin induces biphasic activity in C-fibers in the rat. *Neurosci. Lett.* **208**, 45–48.

Merlos M., Giral M., Balsa D., Ferrando R., Queralt M., Puigdemont A., Garcia-Rafanell J. and Forn J. (1997) Rupatadine, a new potent, orally active dual antagonist of histamine and platelet-activating factor (PAF). *J. Pharmacol. Exp. Ther.* **280**, 114–121.

Montrucchio G., Alloatti G. and Camussi G. (2000) Role of platelet-activating factor in cardiovascular pathophysiology. *Physiol. Rev.* **80**, 1669–1699.

Morita K., Morioka N., Abdin J., Kitayama S., Nakata Y. and Dohi T. (2004) Development of tactile allodynia and thermal hyperalgesia by intrathecally administered platelet-activating factor in mice. *Pain* **111**, 351–359.

Nakasaki T., Masuyama K., Fukui H., Ogino S., Eura M., Samejima Y., Ishikawa T. and Yumoto E. (1999) Effects of PAF on histamine H1 receptor mRNA expression in rat trigeminal ganglia. *Prostaglandins Other Lipid Mediat.* **58**, 29–41.

Nakatsuka T., Park J. S., Kumamoto E., Tamaki T. and Yoshimura M. (1999) Plastic changes in sensory inputs to rat substantia gelatinosa neurons following peripheral inflammation. *Pain* **82**, 39–47.

Nakatsuka T., Ataka T., Kumamoto E., Tamaki T. and Yoshimura M. (2000) Alteration in synaptic inputs through C-afferent fibers to substantia gelatinosa neurons of the rat spinal dorsal horn during postnatal development. *Neuroscience* **99**, 549–556.

Nichols M. L., Allen B. J., Rogers S. D. *et al.* (1999) Transmission of chronic nociception by spinal neurons expressing the substance P receptor. *Science* **286**, 1558–1561.

Noguchi K., Morita I. and Murota S. (1989) The detection of platelet-activating factor in inflamed human gingival tissue. *Arch. Oral Biol.* **34**, 37–41.

Obata K. and Noguchi K. (2004) MAPK activation in nociceptive neurons and pain hypersensitivity. *Life Sci.* **74**, 2643–2653.

Pitcher G. M. and Henry J. L. (2002) Second phase of formalin-induced excitation of spinal dorsal horn neurons in spinalized rats is reversed by sciatic nerve block. *Eur. J. Neurosci.* **15**, 1509–1515.

Prescott S. M., Zimmerman G. A., Stafforini D. M. and McIntyre T. M. (2000) Platelet-activating factor and related lipid mediators. *Annu. Rev. Biochem.* **69**, 419–445.

Puig S. and Sorkin L. S. (1996) Formalin-evoked activity in identified primary afferent fibers: systemic lidocaine suppresses phase-2 activity. *Pain* **64**, 345–355.

Sakurada T., Wako K., Sugiyama A., Sakurada C., Tan-No K. and Kisara K. (1998) Involvement of spinal NMDA receptors in capsaicin-induced nociception. *Pharmacol. Biochem. Behav.* **59**, 339–345.

South S. M., Kohno T., Kaspar B. K. *et al.* (2003) A conditional deletion of the NR1 subunit of the NMDA receptor in adult spinal cord dorsal horn reduces NMDA currents and injury-induced pain. *J. Neurosci.* **23**, 5031–5040.

Teather L. A., Magnusson J. E. and Wurtman R. J. (2002) Platelet-activating factor antagonists decrease the inflammatory nociceptive response in rats. *Psychopharmacology (Berl)* **163**, 430–433.

Thornton P. D., Gerke M. B. and Plenderleith M. B. (2005) Histochemical localisation of a galactose-containing glycoconjugate expressed by sensory neurones innervating different peripheral tissues in the rat. *J. Peripher. Nerv. Syst.* **10**, 47–57.

Tjolsen A., Berge O. G., Hunskaar S., Rosland J. H. and Hole K. (1992) The formalin test: an evaluation of the method. *Pain* **51**, 5–17.

Tsuda M., Ueno S. and Inoue K. (1999a) In vivo pathway of thermal hyperalgesia by intrathecal administration of alpha,beta-methylene ATP in mouse spinal cord: involvement of the glutamate-NMDA receptor system. *Br. J. Pharmacol.* **127**, 449–456.

Tsuda M., Ueno S. and Inoue K. (1999b) Evidence for the involvement of spinal endogenous ATP and P2X receptors in nociceptive responses caused by formalin and capsaicin in mice. *Br. J. Pharmacol.* **128**, 1497–1504.

Tsuda M., Koizumi S., Kita A., Shigemoto Y., Ueno S. and Inoue K. (2000) Mechanical allodynia caused by intraplantar injection of P2X receptor agonist in rats: involvement of heteromeric $P2X_{2/3}$ receptor signaling in capsaicin-insensitive primary afferent neurons. *J. Neurosci.* **20**, RC90 (1–5).

Tsuda M., Shigemoto-Mogami Y., Koizumi S., Mizokoshi A., Kohsaka S., Salter M. W. and Inoue K. (2003) $P2X_4$ receptors induced in spinal microglia gate tactile allodynia after nerve injury. *Nature* **424**, 778–783.

Wheeler-Aceto H., Porreca F. and Cowan A. (1990) The rat paw formalin test: comparison of noxious agents. *Pain* **40**, 229–238.

Yoshimura M. and Jessell T. M. (1989) Primary afferent-evoked synaptic responses and slow potential generation in rat substantia gelatinosa neurons in vitro. *J. Neurophysiol.* **62**, 96–108.

Yoshimura M. and Nishi S. (1993) Blind patch-clamp recordings from substantia gelatinosa neurons in adult rat spinal cord slices: pharmacological properties of synaptic currents. *Neuroscience* **53**, 519–526.

Zhuang Z. Y., Xu H., Clapham D. E. and Ji R. R. (2004) Phosphatidylinositol 3-kinase activates ERK in primary sensory neurons and mediates inflammatory heat hyperalgesia through TRPV1 sensitization. *J. Neurosci.* **24**, 8300–8309.

Role of platelet-activating factor in pneumolysin-induced acute lung injury

Martin Witzenrath, MD; Birgitt Gutbier; John S. Owen, PhD; Bernd Schmeck, MD; Timothy J. Mitchell, PhD; Konstantin Mayer, MD; Michael J. Thomas, PhD; Satoshi Ishii, PhD; Simone Rosseau, MD; Norbert Suttorp, MD; Hartwig Schütte, MD

Objective: **Acute respiratory failure is a major complication of severe pneumococcal pneumonia, characterized by impairment of pulmonary microvascular barrier function and pulmonary hypertension. Both features can be evoked by pneumolysin (PLY), an important virulence factor of *Streptococcus pneumoniae*. We hypothesized that platelet-activating factor (PAF) and associated downstream signaling pathways play a role in the PLY-induced development of acute lung injury.**

Design: **Controlled, *ex vivo* laboratory study.**

Subjects: **Female Balb/C mice, 8–12 wks old.**

Interventions: **Ventilated and blood-free–perfused lungs of wild-type and PAF receptor–deficient mice were challenged with recombinant PLY.**

Measurements and Main Results: **Intravascular PLY, but not the pneumolysoid Pd-B (PLY with a Trp-Phe substitution at position 433), caused an impressive dose-dependent increase in pulmonary vascular resistance and increased PAF in lung homogenates, as detected by reversed-phase high-performance liquid chromatography coupled to tandem mass spectrometry. The pressor response was reduced in lungs of PAF receptor–deficient mice and after PAF receptor blockade by BN 50730. PLY and exogenous PAF increased thromboxane B2 in lung effluate, and thromboxane receptor inhibition by BM 13505 diminished the pressor response to PLY. Differential inhibition of intracellular signaling steps suggested significant contribution of phosphatidylcholine-specific phospholipase C and protein kinase C and of the Rho/Rho-kinase pathway to PLY-induced pulmonary vasoconstriction. Unrelated to the pulmonary arterial pressor response, microvascular leakage of PLY was diminished in lungs of PAF receptor–deficient mice as well.**

Conclusions: **PAF significantly contributed to PLY-induced acute injury in murine lungs. The PAF-mediated pressor response to PLY depends on thromboxane and on the downstream effectors phosphatidylcholine-specific phospholipase C, protein kinase C, and Rho-kinase. (Crit Care Med 2007; 35:1756–1762)**

KEY WORDS: pneumococcal pneumonia; pneumolysin; acute lung injury; isolated mouse lung; platelet activating factor; thromboxane; Rho-kinase

Community-acquired pneumonia is an important cause of morbidity and mortality. Acute respiratory failure and sepsis are significant complications of severe community-acquired pneumonia and may result in acute respiratory distress syndrome, which is characterized by microvascular leakage and pulmonary hypertension (1). *Streptococcus pneumoniae* is the most prevalent causal pathogen identified in community-acquired pneumonia (2). Pneumolysin (PLY), a cytoplasmic 53-kDa protein toxin, is an important virulence factor of *S. pneumoniae* (3, 4). PLY is produced by all clinical isolates and released during pneumococcal lysis. Bacteremia frequently occurs in pneumococcal pneumonia, and purified human anti-PLY immunoglobulin G protected mice against bacteremic pneumococcal disease and increased survival (5). Moreover, studies with a PLY-negative mutant of *S. pneumoniae* suggested a critical role of PLY in acute pneumococcal sepsis (6). Recently, we observed that intravascular PLY induced hyperpermeability and a massive, rapid, and dose-dependent increase of vascular resistance in isolated mouse lungs (7). These findings provided further evidence that PLY may play an important role in the development of acute lung injury in pneumococcal bacteremia and sepsis. However, the mechanisms contributing to these PLY-induced alterations remain unclear.

Platelet-activating factor (PAF) is a potent lipid mediator implicated in diverse inflammatory disorders, including acute respiratory distress syndrome and sepsis (8). Effects of PAF are exclusively mediated by the PAF receptor (PAF-R), which is expressed in many tissues, including the lungs (9). Pulmonary actions of PAF induce both vascular hyperpermeability and vasoconstriction (8, 10). The present study was designed to test the hypothesis

From the Department of Internal Medicine/Infectious Diseases and Respiratory Medicine, Charité-Universitätsmedizin Berlin, Germany (MW, BG, BS, SR, NS, HS); Department of Biochemistry, Wake Forest University School of Medicine, Winston-Salem, NC (JSO, MJT); Division of Infection and Immunity, Glasgow Biomedical Research Centre, University of Glasgow, UK (TJM); Lung Center, Department of Internal Medicine II, University of Giessen, Germany (KM); and the Department of Biochemistry and Molecular Biology, University of Tokyo, Japan (SI).

The authors have no financial interests to disclose.

Parts of this work contribute to the doctoral thesis of Gutbier.

Supported, in part, by grants from the Bundesministerium für Bildung und Forschung to Drs. Schmeck, Rosseau, and Suttorp (CAPNETZ, Competence Network Community-Acquired Pneumonia).

For information regarding this article, E-mail: hartwig.schuette@charite.de

DOI: 10.1097/01.CCM.0000269212.84709.23

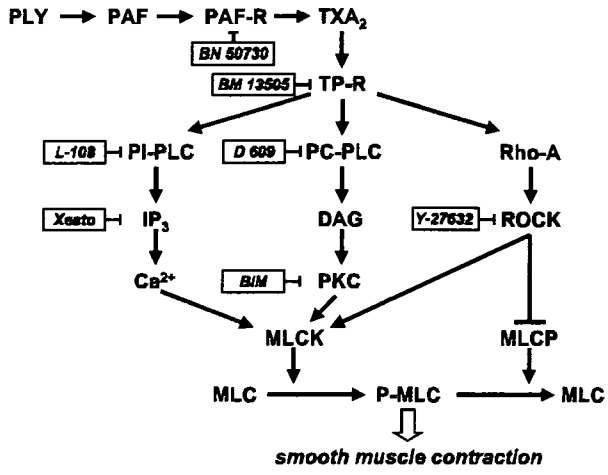

Figure 1. Schematic overview of investigated signaling cascades and employed antagonists. *PLY*, pneumolysin; *PAF*, platelet-activating factor; *PAF-R*, PAF receptor; *TXA_2*, thromboxane A_2; *TP-R*, TXA_2-receptor; *PI-PLC*, phosphatidylinositol-specific phospholipase C; *PC-PLC*, phosphatidylcholine-specific PLC; *IP_3*, inositol trisphosphate; *DAG*, diacylglycerol; *ROCK*, Rho-kinase; *PKC*, protein kinase C; *MLC*, myosin light chain; *MLCK*, MLC kinase; *MLCP*, MLC phosphatase; *P-MLC*, phosphorylated MLC. *BN 50730*, PAF receptor antagonist; *BM 13505*, daltroban, TP-R antagonist; *L-108*, PI-PLC inhibitor; *D 609*, PC-PLC inhibitor; *Xesto*, xestospongin C, inositol trisphosphate antagonist; *BIM*, bisindolylmaleimide, PKC inhibitor; *Y-27632*, ROCK inhibitor.

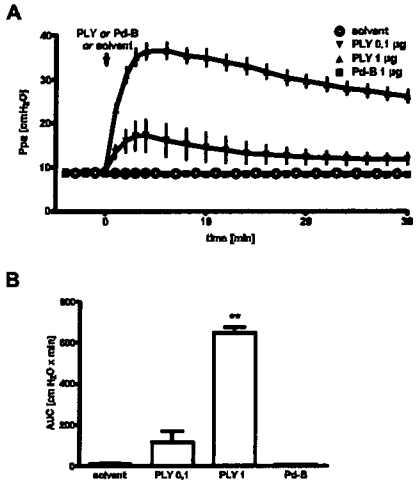

Figure 2. Intravascular pneumolysin (*PLY*), but not Pd-B, induced pulmonary hypertension. PLY (total dose of 0.1 µg or 1.0 µg, respectively), Pd-B (1.0 µg), or solvent were infused via the pulmonary artery within 1 min. *A*, PLY-induced increase of the mean pulmonary arterial pressure (*Ppa*). n = 5 separate experiments per group. *B*, the area under the Ppa curve (*AUC*) markedly increased after PLY but not after Pd-B application. n = 5 per group; $^{**}p < .01$ vs. all other groups.

that PAF and its downstream signaling pathways contribute to PLY-induced impairment of pulmonary hemodynamics and fluid balance.

METHODS

Animals. All animal procedures were approved by the State Office of Health and Social Affairs. PAF-R–deficient mice (PAF-$R^{-/-}$) (11) were backcrossed at least ten times to a Balb/C background. Wild-type (WT) mice were obtained from Charles River (Sulzfeld, Germany).

Isolated Perfused Mouse Lung. Lungs were prepared as described (7, 12), perfused with 37°C sterile Krebs-Henseleit-hydroxyethylamylopectine buffer and ventilated by negative pressure. Pulmonary arterial pressure (Ppa) was continuously monitored. Recombinant PLY, a 53-kDa protein (13), or Pd-B, a mutant PLY protein with a single amino acid substitution at residue number 433 (14), were infused for 1 min into the pulmonary artery or aerosolized into the trachea. For measurement of alveolocapillary permeability, human serum albumin was admixed to the perfusate (0.04%) before toxin application. Bronchoalveolar lavage was performed 30 mins after toxin challenge, and the human serum albumin concentration was measured in bronchoalveolar lavage supernatant (15).

To analyze the role of PAF-related signal transduction pathways in PLY-induced lung injury, we employed different specific inhibitors and antagonists, as summarized in Figure 1. Agents were obtained from the following sources: xestospongin C and L-108 from Biomol (Hamburg, Germany); bisindolylmaleimide, Y-27632, and U46619 from Calbiochem (Darmstadt, Germany); D-609 from Sigma (Deisenhofen, Germany); BM 13505 from Boehringer (Mannheim, Germany); and BN 50730 from Institut Henri Beaufour (Les Ulis, France).

Extraction and Assay of PAF. Lungs were snap frozen 5 mins after PLY infusion, pulverized, weighed, and stored at −80°C. Homogenates were incubated essentially as described (16). Delipidated solids were removed by centrifugation and reserved for total protein assay. After separation (16), the chloroform phase of the solvent was transferred to a fresh tube, and the methanolic phase was washed with 4 mL of chloroform. Both chloroform extracts were pooled, evaporated under a stream of argon, and reconstituted in 1 mL of chloroform/methanol (1:1 vol/vol). Perfusate samples were frozen at −80°C, lipids were extracted in the presence of d3-PAF, and lipid extracts were assayed for total phosphorus and for PAF as described (16). Briefly, PAF was isolated from the lipid extracts by preparative normal-phase high-performance liquid chromatography and quantified using reversed-phase high-performance liquid chromatography coupled to tandem mass spectrometry in the multiple-reaction monitoring mode (16). Delipidated solids from lung homogenates were air-dried, digested, and assayed for total protein, essentially as described (17). The internal standard for PAF measurement, d3-PAF, was synthesized as described (18). Other PAF standards were purchased from Avanti (Alabaster, AL) or from Bachem (King of Prussia, PA).

Thromboxane Quantification. Thromboxane A2 (TXA_2) in perfusion buffer samples was assessed as the stable degradation product TXB_2 by enzyme immunoassay (Cayman Chemicals, Ann Arbor, MI).

Data Analysis. Data are expressed as mean ± SEM. Differences were analyzed by Mann-Whitney U test or one-way analysis of variance followed by *post hoc* Tukey test. All calculations were performed with GraphPad 4 Software (San Diego, CA).

RESULTS

Conserved Undecapeptide Sequence of PLY Accounted for the Pressor Response. Perfusion of isolated WT mice lungs with PLY induced a rapid and dose-dependent Ppa increase (Fig. 1). In contrast, perfusion with the pneumolysoid Pd-B did not alter Ppa (Fig. 2).

PAF and TXA_2 Contributed to PLY-Induced Pulmonary Hypertension. After PLY infusion, PAF content in the venous effluate was below the detection limit. However, in mouse lung tissue, PAF content was significantly increased after PLY infusion (Fig. 3*A*). The PLY-induced Ppa increase was significantly lower in PAF-$R^{-/-}$ compared with WT mice lungs (Fig. 3, *B* and *C*). Baseline Ppa values did not differ between the two groups (WT, 8.83 ± 0.23 cm H_2O; PAF-$R^{-/-}$, 8.30 ± 0.34 cm H_2O), and the dose-dependent vasopressor responses to the thromboxane analogue U46619 did not differ between PAF-$R^{-/-}$ mice and WT mice (maximum delta Ppa to 100 nM U46619: WT, 12.7 ± 0.9 cm H_2O; PAF-$R^{-/-}$, 10.85 ± 2.1 cm H_2O). Moreover, the PAF-R antagonist BN 50730 diminished

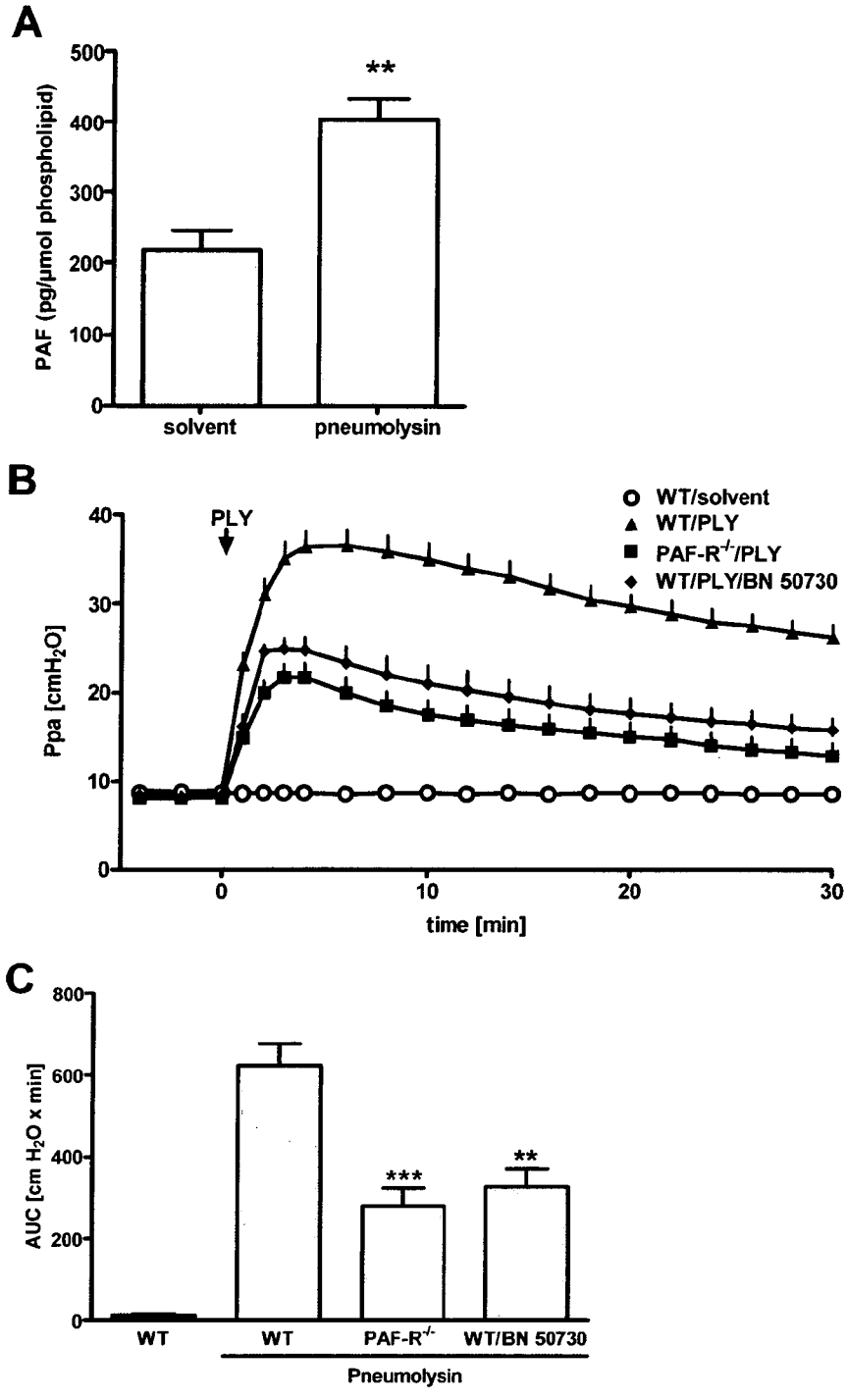

Figure 3. Pulmonary hypertension evoked by pneumolysin (*PLY*) was partly mediated by platelet-activating factor (*PAF*). *A*, PAF was increased in homogenized lung tissue of wild-type (*WT*) mice after PLY infusion as compared with untreated lungs (*solvent*). PAF was measured by reversed-phase high-performance liquid chromatography coupled to tandem mass spectrometry, and PAF levels were related to total lung phospholipids. n = 7 per group; $^{**}p < .01$. *B* and *C*, PLY (1 µg/min) or solvent was infused at t = 0 min for 1 min. Pulmonary arterial pressure (*Ppa*; *B*) and the area under the Ppa curve (*AUC*) values (*C*) were diminished in PLY-challenged lungs of PAF receptor–deficient mice (*PAF-R$^{-/-}$/PLY*) and in WT lungs preperfused with the PAF-R antagonist BN 50730 (10 µM) starting at t = −15 mins (*WT/PLY/BN 50730*) compared with PLY-challenged WT lungs (*WT/PLY*). WT/solvent, n = 5; WT/PLY, n = 8; PAF-R$^{-/-}$/PLY, n = 7; WT/PLY/BN 50730, n = 6. $^{**}p < .01$ vs. WT/PLY; $^{***}p < .001$ vs. WT/PLY.

the pressor response to PLY in lungs of WT mice (Fig. 3, *B* and *C*).

Perfusion of WT mice lungs with PLY induced a significant increase of thromboxane in the venous effluate (Fig. 4*A*). Increase of Ppa and TXA_2 generation was also induced by PAF perfusion (Fig. 4, *A* and *B*). Preperfusion with the specific thromboxane receptor antagonist BM 13505 strongly reduced the PLY-induced pressor response (Fig. 4*C*). A moderate reduction of this pressor response was also observed in lungs preperfused with the 5-lipoxygenase inhibitor AA-861 (10 µM; area under the curve 441.1 ± 49.6 cm H_2O × min, n = 5).

Phosphatidylcholine-Specific Phospholipase C and Protein Kinase C, but Not Phosphatidylinositol-Specific Phospholipase C and Inositol Trisphosphate, Contributed to PLY-Induced Intracellular Signal Transduction. TXA_2 and leukotrienes may contribute to acute pulmonary vasoconstriction via G-coupled receptors linked to phospholipase C (PLC). Pretreatment of perfused lungs with the phosphatidylcholine-specific PLC inhibitor D-609, but not with the phosphatidylinositol-specific PLC inhibitor L-108, largely attenuated the pressor responses to PLY (Fig. 5). Inhibition of the downstream effector of phosphatidylinositol-specific PLC, inositol trisphosphate (IP_3), using the IP_3 receptor antagonist xestospongin C, did not affect PLY-induced vasoconstriction (Fig. 5). In contrast, the selective inhibitor of the phosphatidylcholine-specific PLC downstream effector protein kinase C (PKC), bisindolylmaleimide, largely attenuated PLY-induced vasoconstriction.

Role of Rho-Kinase for PLY-Induced Pressor Response. Inhibition of Rho-kinase by Y-27632 resulted in a distinct reduction of Ppa increase (Fig. 5). Moreover, combined pretreatment with bisindolylmaleimide and Y-27632 had a significantly greater effect than each of the inhibitors and almost completely abolished the PLY-induced vasoconstriction, suggesting an additive role for Rho-kinase besides the PKC pathway.

PAF Contributed to PLY-Induced Hyperpermeability. PLY infusion increased isolated lung permeability (Fig. 6*A*). Moreover, aerosolized PLY evoked lung hyperpermeability (Fig. 6*B*) but did not alter Ppa (area under the curve: control, 17.28 ± 4.3 cm H_2O × min; 1 µg of PLY, 15.30 ± 6.1 cm H_2O × min; n = 6). Hyperpermeability due both to PLY infu-